JPL Publication 83-82

(NASA-CR-173742) REQUIREMENTS FOR A TRANSFORMERLESS POWER CONDITIONING SYSTEM (Jet Propulsion Lab.) 96 p HC A05/MF A01 N84-27981
CSCL 10B Unclas
G3/33 19798

Requirements for a Transformerless Power Conditioning System

J. Klein
T. Koerner
W. Rippel
J. Kalbach

March 1984

Prepared for
Sandia National Laboratories,
U.S. Department of Energy
Through an Agreement with
National Aeronautics and Space Administration
by
Jet Propulsion Laboratory
California Institute of Technology
Pasadena, California

JPL Publication 83-82

Requirements for a Transformerless Power Conditioning System

J. Klein
T. Koerner
W. Rippel
J. Kalbach

March 1984

Prepared for
Sandia National Laboratories,
U.S. Department of Energy
Through an Agreement with
National Aeronautics and Space Administration
by
Jet Propulsion Laboratory
California Institute of Technology
Pasadena, California

Prepared by the Jet Propulsion Laboratory, California Institute of Technology, for Sandia National Laboratories, U.S. Department of Energy, through an agreement with the National Aeronautics and Space Administration.

Work conducted through NASA Task RE-152, Amendment 325, Sandia Order No. 68-4728.

ABSTRACT

Requirements for development of a Transformerless Power Conditioning Subsystem (TPCS) that will meet utility, manufacturer, and customer needs are detailed in this report. Issues analyzed include current utility guidelines, safety and grounding issues that appear as local codes, various kinds of TPCS connections that can be developed, dc injection, and a brief survey of TPCS circuit topologies that will meet requirements.

The major result of this study is that a finite time exists for control operation before dc injection into the distribution transformer causes customer outage (on the order of seconds). This time permits the control system to sense a dc injection condition and remove the TPCS from the utility system. Requirements for such a control system are specified.

The study also showed that a three-wire connection will ensure balanced operation for customer loads and that two-wire connections caused average value dc to be injected into single-phase loads. This type of connection also allows for the lowest array voltage.

The conclusion from the study is that requirements for a TPCS can be determined and that there are no "showstopping" issues preventing implementation. The actual design and topology of the TPCS has been left for further study.

CONTENTS

Figures

Figures

Tables

Tables

Part One
Executive Summary

EXECUTIVE SUMMARY

Photovoltaic (PV) energy production has evolved from an interesting research phenomena to an accepted method of energy production. In the early years of development, money and effort was (and still is being) spent on ways to lower the cost of the PV cells and arrays. Later, monies were spent on the individual subsystems. Of these, power conditioning and utility interface have become a major part of the U.S. Department of Energy (DOE) program.

This report discusses the development of a Transformerless Power Conditioning Subsystem (TPCS) that might be more efficient and less costly to produce. The end result of such a program will be in the integration of a TPCS into the utility system. To do this, utilities will need proof that these subsystems can operate in a utility environment in a safe and reliable manner. Therefore, the recommendations presented in this report are for a system that will be easily accepted by the utility industry and then installed on a system.

To set forth the requirements for a TPCS, the concerns as expressed by utilities, manufacturers, and consumers must be explored. Table 1 summarizes the areas of concern and suggests possible solutions. Figure 1 shows a possible on-line diagram that incorporates the following concerns and solutions:

(1) Current Utility Practices. Current utility practices vary from utility to utility. The specific requirements upon the PV installer are not specific. Some utilities require isolation transformers while others prefer the use of dedicated distribution transformers to solve perceived problems. The discussions and analyses presented in this report tend to negate these concerns. Each concern is reviewed and a possible solution is presented.

(2) Direct Current Injection. The principal issue associated with a TPCS involves the question of dc Injection. After detailed analysis, it was found that a finite amount of time transpired from the failure of the PCS until (1) saturation of the distribution transformer occurred, and (2) the primary fused cutout would open, if at all. The solution of this problem involves the development of a control system that senses dc injection and operates a contactor and crowbar internal to the TPCS.

(3) Customer Transformers (Saturation). A second issue involves the effect of a TPCS on customer transformers (saturation). Because two-wire systems (in which the single-phase load is connected between a hot leg and ground) lead to average value dc injected into the customer load, a three-wire connection for the inverter is recommended.

(4) Ground Loops. Ground loops are always a concern in any installation. The various applicable codes are quite specific about requirements. Because lightning protection and solid grounding are required at the array and because the code allows for grounding physically remote but electrically close to the array, a current carrying neutral tied to the house ground is recommended. To provide lightning protection, a spark gap or lightning arrestor is used that only grounds the array under transient conditions.

(5) Safety. Personnel safety is another issue addressed by the study. To reduce the array voltage to ground that a consumer or maintenance personnel might contact, a three-wire array connection with current carrying neutral (see discussion under Ground Loops) is recommended. Ground-Fault Interrupters (GFIs) are not required by code for single-phase PV installations.

(6) Optimum Topology. The issue of optimum topology is one for the designer of the TPCS system. If flexibility is required in the installation of interest, then a topology where dc injection is prohibited and any array voltage is accommodated is necessary. If, on the other hand, the array voltage is designed to exceed the worst-case utility line voltage and simplicity of design is desired, then a simple modulated bridge might be a wise choice.

Once these issues have been resolved, then they must be reexamined in light of the possibility of multiple users on a single utility distribution transformer. The issues here include increased outages and complaints due to interference and transients from the PV source, multiple ground loops between residences, and the use of a dedicated distribution transformer to alleviate these concerns. The array connections and control schemes discussed in this report negate the need for such additional utility equipment. By controlling the dc injection, the ground loop paths, and the transient conditions of the PCS, little reference, if any, will be seen between customers.

In conclusion, a transformerless PCS can be developed that will meet all the concerns of all parties involved. It should have characteristics that please the consumer and manufacturer; it should be safe, highly efficient, and cheaper to build and buy. At the same time, a transformerless PCS will meet the necessary requirements of the utilities who wish to protect themselves and other non-PV customers.

Table 1. Issues and Solution Summary

Concern	Study Findings	Solution
Direct Current Injection of Distribution Transformer		Sense 1%
	Finite time to saturation	0.1% sensitivity
	Finite time to fuse open	3 s to contact open crowbar array concurrently
Customer Load Saturation	Two-wire connection leads to average value dc on customer loads	Three-wire connection for inverter
Ground Loops	Code requires lightning protection	Current carrying neutral tied to house ground
	Code requires solid array grounding	Lightning arrestor ties array to ground at array
	Code allows array grounding at meter pan	
Safety	Excessive array voltage	Three-wire dc array connection with current carrying neutral
Current Utility Practices	Guidelines not specific	Array connection, control schemes will negate need for isolation transformer
	Isolation transformer may be required	
	Dedicated transformer is preferred usage	Inverter connection, control scheme negate need for dedicated transformer
Multiple Ground Paths	Interference between customers	Control scheme eliminates interference
Multiple Customers on one Utility Transformer	Increased outages	Control scheme reduces outages
	Increased customer complaints	Control scheme reduces customer complaints

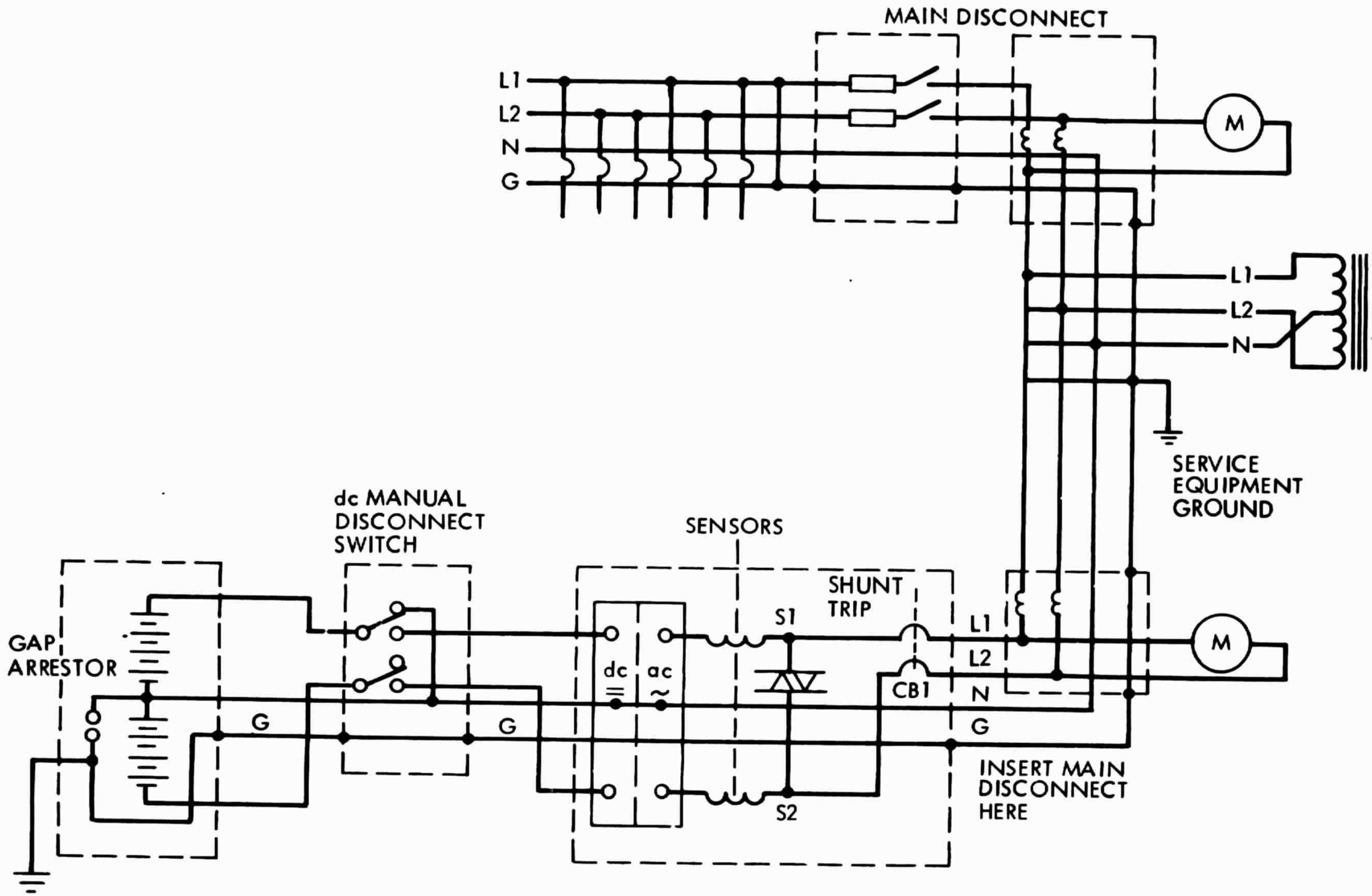

Figure 1. Detailed Schematic for Interconnection

Part Two
Requirements

SECTION I

INTRODUCTION

Photovoltaic (PV) energy production has evolved from an interesting research phenomena to an accepted method of energy production. In the early years of development, money and effort was (and still is being) spent on ways to lower the cost of the PV cells and arrays. Later, monies were spent on the individual subsystems. Of these, power conditioning and utility interface have become a major part of the U.S. Department of Energy (DOE) program.

In 1979, four contracts were awarded by DOE to look at advanced power conditioning and the cost of interfacing to a utility. Each of these designs utilized an isolation transformer in the design. While one contractor was able to substantially reduce the size and weight of the transformer, the transformer was still a major cost and loss component of the overall design.

This report discusses the development of a Transformerless Power Conditioning Subsystem (TPCS) that might be more efficient and less costly to produce. The end result of such a program will be in the integration of a TPCS into the utility system. To do this, utilities will need proof that these subsystems can operate in a utility environment in a safe and reliable manner. Therefore, the recommendations presented in this report are for a system that will be easily accepted by the utility industry and then installed on a system. The Residential Experiment Station (RES) sites might be an appropriate place for the installation of such prototypes. From the experience gained at these sites, design simplifications can be made that will reduce the cost even further without degrading the service of the original prototype.

For purposes of this study, a generic system design was developed that meets the concerns of all parties involved: utilities, manufacturers, and consumers. Thus, present designs may or may not meet the guidelines and requirements as set down by the various parties. It is not the intent of this document to present the "one and only" design but to show that a possible TPCS design does exist. It is left up to others to use the information presented to determine the "optimum" TPCS design. To set forth the requirements for a TPCS, the concerns as expressed by utilities, manufacturers, and consumers are discussed in detail. The utility concerns are presented in Section II, where the issues of isolation, grounding, and dedicated distribution transformer usage are discussed. Then a brief discussion of existing guidelines concerning these utility issues is presented.

Section III discusses the consumer viewpoint by reviewing pertinent documents, including appropriate sections from the 1984 National Electric Code (NEC) and a new guideline document prepared by Underwriters Laboratories (UL).

The manufacturer's concerns are presented in Section IV, which analyzes various transformerless topologies. Such issues as stresses, losses, failure modes, and waveshapes are presented so that the tradeoffs for TPCS selection are evident.

The impact of dc current injection transformers is presented in Section V, where detailed analyses are presented that show the time frame of concern for sensing and clearing dc injection. Analysis is also presented that shows the effects of dc injection on transformer size. This information determines the control (protection) requirements for a TPCS.

The final three sections discuss the overall system aspects of individual concerns. Section VI shows generic wiring diagrams for a two- and three-wire system that will meet the safety and grounding concerns. A brief discussion of control operation is presented. Section VII lists a set of generic recommendations. This section discusses the choice of a three-wire system, two possible topologies that have good isolation characteristics, and the control requirements for an acceptable TPCS. Finally, Section VIII lists the conclusions for this report, including deficiencies in the guidelines and requirements as well as suggested steps to place and test a Transformerless Power Conditioning Subsystem in the field.

SECTION II

UTILITY GUIDELINES

A number of documents have been written recently concerning the interconnection of small power producers to the electric utility. In an effort to compile all of the concerns into a unified document, a major effort was initiated by the Electric Power Research Institute (EPRI) and the U.S. Department of Energy Office (DOE) of Photovoltaic Systems through the Jet Propulsion Laboratory (JPL) to clarify the issues.[1] A set of functional requirements was discussed that reflect the inputs of over 80 manufacturers and utilities. The areas discussed include:

(1) Isolation.

(2) Grounding.

(3) Distribution Transformers.

(4) Load-Break Disconnects.

(5) Synchronization.

(6) Startup.

(7) Voltage.

(8) Loss of Utility and Recovery.

(9) Voltage Flicker.

(10) Harmonics.

(11) Reactive Power.

(12) Electromagnetic Interference.

Isolation, grounding, and distribution transformers are applicable to an understanding of utility guidelines for transformer usage. While the others affect choices of topology, photovoltaic array working voltage range, and means for control of the inverter, much effort and money have already been spent studying them and will not be discussed in detail here.

A. BACKGROUND

To provide a background for some of the technical issues in the design of a "transformerless" power conditioning subsystem, a summary of the functions of a transformer in a solar photovoltaic system follows.

An isolating transformer installed between the conditioner's inverter output circuit and the utility's ac system is capable of performing at least four useful functions. These are listed below together with examples

---

[1] Interconnecting DC Energy Systems: Responses to Technical Issues, EPRI AP/EMM-3124, Special Issues Assessment 82-412, June 1983.

of how each function can be performed without a transformer. The proposed alternatives are not necessarily the only alternatives.

1. Voltage Transformation

Voltage transformation gives the photovoltaic system designer a wide choice of array and inverter direct current (dc) operating voltages. By selecting an appropriate primary-to-secondary fixed turns ratio, the array's working dc voltage can be selected independently of the utility line's alternating current (ac) voltage.

In a transformerless subsystem, the utility line voltage may dictate the photovoltaic array configuration and number of cells in series. Alternatively, there are inverter topologies in which the dc array voltage can be lower than the utility circuit's peak voltage.

2. Ground Fault and Leakage Current Path Control

Because they are electrically isolated by a transformer, the primary and secondary circuits can be independently grounded, following the electrical code for separately derived power systems to avoid unwanted ground loops and ground current.

Without an isolating transformer, the photovoltaic subsystem does not become a separately derived power source. The photovoltaic and utility power systems would then require solidly interconnected neutral conductors (if neutral is used) and a single grounding point at the building entrance service equipment for the interconnected neutrals.

3. Isolation to Keep dc out of Utility Circuits

Residual dc from unbalanced components or a fault within the power conditioner could cause dc to flow in the power circuits to which it is directly connected. If allowed to continue, this could cause saturation problems in magnetic devices such as induction motors and transformers served by the utility, as well as the utility distribution transformer itself. The possibility of overheating these devices or causing overcurrent protection to interrupt service could affect all customers served by a utility transformer.

An isolating transformer that has been designed to tolerate the anticipated amount of dc, and which will block dc from flowing in circuits beyond the transformer, is one solution. Such transformers differ from typical utility distribution transformers because they are constructed with a small air gap in the core assembly. They have substantially higher magnetizing current and losses than typical distribution transformers.

Without a transformer in the conditioning subsystem, the proper performance of the utility transformer and other loads connected in parallel with the conditioning system will depend upon controls in the conditioning subsystem to limit the dc to acceptable levels or to interrupt the interconnection between the conditioner and the utility circuit if automatic controls fail to keep the dc at acceptable levels.

4. Noise Filtering

Internal leakage inductance is an inherent characteristic of power transformers. It is created by the imperfect coupling of primary and secondary circuits and acts as the equivalent of a series-connected inductor. Using capacitors on the transformer input, output, or both input and output, the combination becomes the equivalent of a low-pass filter that can reduce unwanted conducted electrical noise and impulse currents from passing through this interface.

Even with a transformer enhanced with capacitors to act as a filter (typically most effective in the range of 10 to about 500 kHz), supplementary line filtering may be required. Without a transformer, line filters may be required to do the entire job.

B. ISOLATION

Electrical isolation between the dc source and the ac system guarantees that dc will not reach the distribution transformer or other loads. Figure 2-1 shows a possible photovoltaic interconnection to a utility system. Notice that the PV source is connected in parallel to the consumer's loads and can be disconnected from the system without affecting the loads. In the diagram an isolation transformer is placed in the output stage of the power conditioning subsystem (PCS), preventing steady-state dc injection into either the customer's loads or the distribution transformer.

In some cases, the isolation transformer is placed internal to the power conditioning unit (PCU) and switching devices (SCRs, transistors, GTOs, etc.), or diodes are placed between the isolation transformer and the distribution transformer. In this instance, a failure in the switching circuits may place a rectifier load across the distribution transformer (Figure 2-2) causing an average value dc load current to flow from the utility system. Thus, the use of an additional transformer does not ensure against the possibility of dc load current, only against the injection of dc array current caused by a failure of the PCS. Injecting dc into the distribution transformer secondary affects the magnetic flux in the core, which could lead to saturation of the core. This highly non-linear situation will cause voltage nonlinearities and possible overcurrents in the power source circuits as a result of high peak magnetizing currents on alternate half cycles. In extreme cases, the primary overcurrent protections for the distribution transformer primary fuse may open, causing customer outages.

C. GROUNDING

The issues of grounding and safety fall under the jurisdiction of the National Electric Code (NEC) and Underwriters Laboratories (UL). These issues are so critical to an understanding of utility requirements that an entire section (Section III) is devoted to them.

D. DEDICATED DISTRIBUTION TRANSFORMER

Solar generation by its nature is many times considered as non-constant generation, that is, its output is a function of the sun or wind. In turn, the output power (both real and reactive) will also vary with time. To reduce these effects on consumers other than the PV owner, some utilities are requiring the use of a pole-top transformer dedicated to the PV owner. While this is an expensive solution, it does isolate the PV system from other customers. In other cases, some utilities are requiring the use of dedicated distribution transformers to minimize customer outage time resulting from PV disconnect procedures. To perform line maintenance, the PV source must be removed electrically from the circuit. One means of disconnecting the PV source is to pull the distribution transformer primary fused cut-out. If a dedicated transformer is not installed, other customers share the same transformer; therefore, their service will be discontinued along with PV owners' even though the feeder from which they receive service might still be energized.

Finally, a dedicated transformer will decrease neighboring customer outage time when a PV-induced transient opens the primary fused cut-out. Other customers remote from the dedicated transformer will not incur an outage due to a PV system fault; however, in no way does the use of a dedicated distribution transformer alleviate the concerns for dc isolation, as previously discussed.

E. EXISTING GUIDELINES

Even though utilities recognize that the aforementioned concerns are real, few have actually required an isolation transformer. A review of about a dozen utility and public utility commission guidelines reveals a preference for the usage of a dedicated distribution transformer. Only one guideline specifically calls for the use of an isolation transformer in addition to the use of a dedicated transformer.

The remainder of this report considers the technical problems and presents possible solutions for the concerns of isolation, dc injection, grounding, and safety. The institutional problem of acceptance must be resolved by individual utilities once sufficient operating experience is logged.

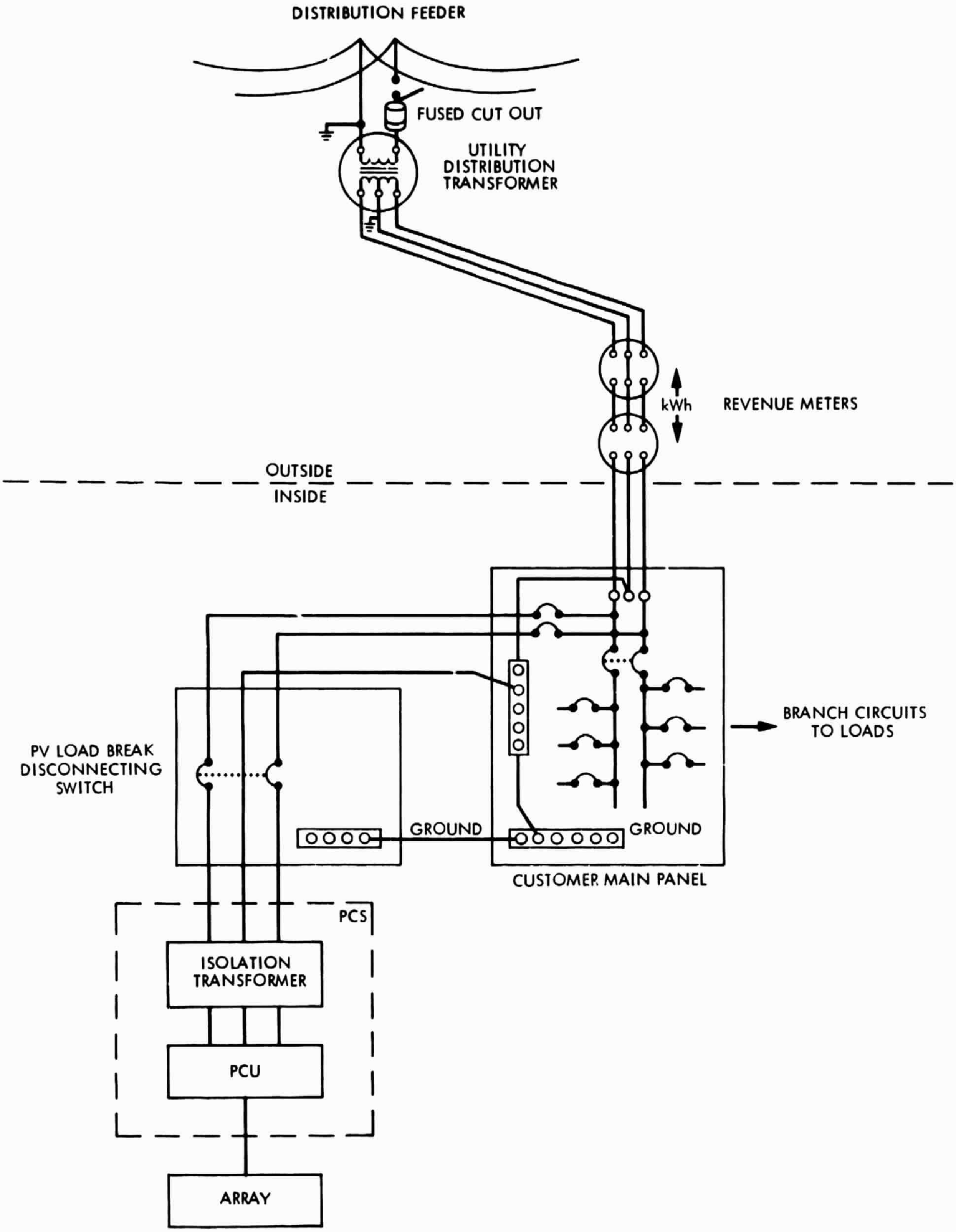

Figure 2-1. Interconnection of Photovoltaic Source to a Utility

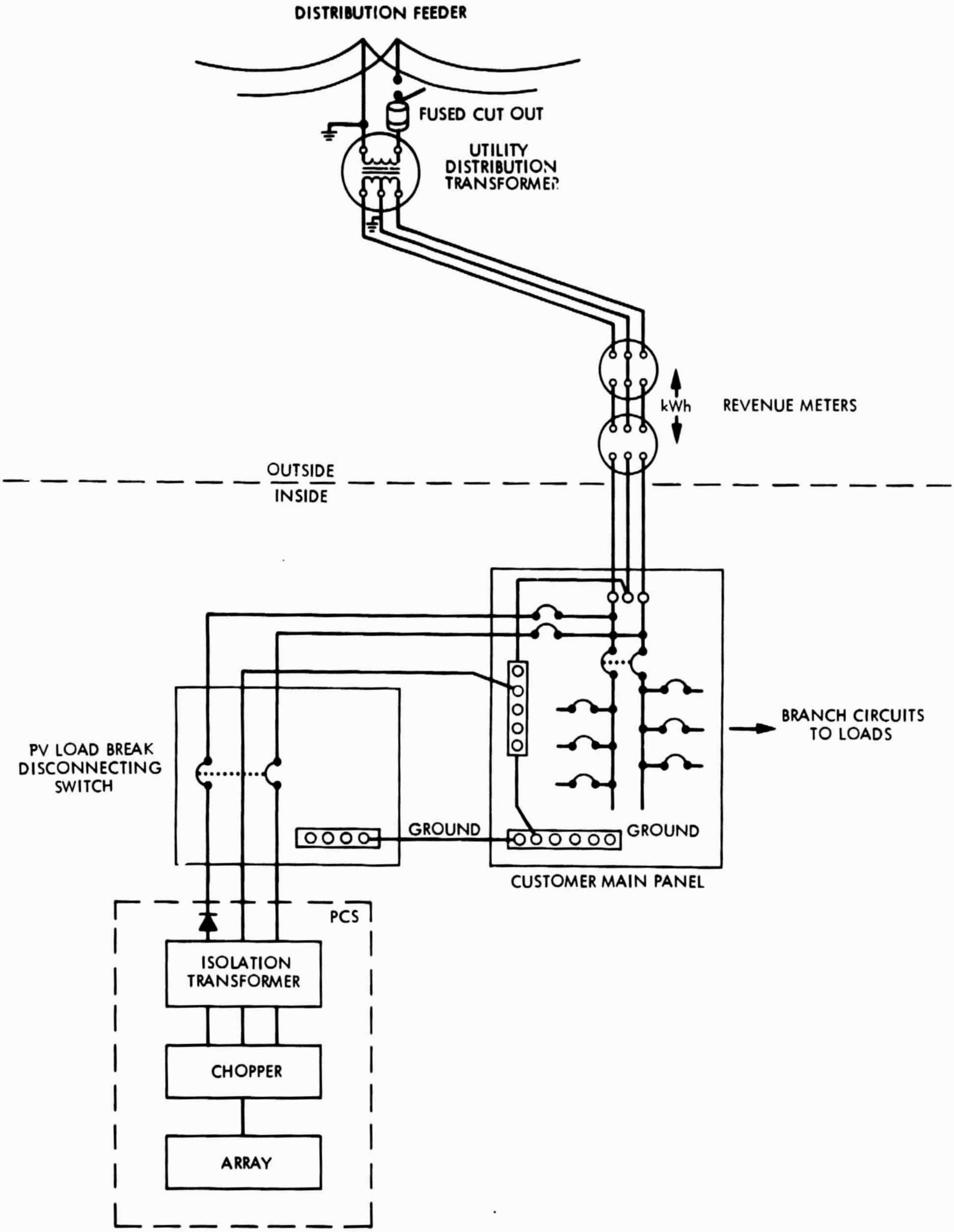

Figure 2-2. Interconnection of a High-Frequency Photovoltaic Source to a Utility

SECTION III

SAFETY AND GROUNDING

A. CODE REQUIREMENTS

Various safety and grounding documents were examined that are applicable to Solar Photovoltaic Systems. These documents are described below.

1. Underwriters Laboratories, Inc.

Underwriters Laboratories, Inc., (UL) Subject 1703 is a proposed First Edition of a UL Standard for Flat-Plate Photovoltaic Modules and Panels, UL 1703. These proposed requirements are of a tentative and early nature for review and comment only. They are not for use in judging the product for compliance with current requirements. However, the assumption can be made that the first version of UL 1703 that is adopted will contain most of these tentative requirements. When completed and approved, UL 1703 will cover the safety requirements for manufactured solar PV flat-plate modules, panels, and arrays. The remaining manufactured units and wiring devices of a PV system, including the dc-to-ac converter/conditioner, controls, and metering and wiring devices, are covered by other UL standards.

2. National Electrical Code ANSI/NFPA 70-1981

Article 210 of the National Electric Code (NEC) regulates the use of ground-fault indicators (GFIs). According to Article 210-8, GFIs are required for 125-V, single-phase installations where ground protection for personnel is required.

Article 250-23 requires the utility ac power source neutral to be grounded where power enters the building. Within the building, the neutral conductor must also be grounded at the secondary output of any transformer or independent power source that is used as a separately derived power source (see ANSI/NFPA 70-1981 Article 250-26).

Proposed Article 690 concerns the installation of complete solar photovoltaic systems. It includes circuit requirements, disconnecting means, wiring methods, grounding, marking, and connection to other sources. Although it is still a proposal, it has been accepted in principle with instructions to the committees to correlate the interconnect requirements of proposed Article 690 with proposed Article 705. Article 690 contains only those details that are specific to PV systems. Other Articles and Sections of the National Electrical Code will still apply if no exception is permitted in Article 690.

3. National Fire Protection Act

Arrays mounted on buildings or ground level supports will be exposed to the direct or indirect effects of lightning. Where lightning is a recognized hazard and where protection is to be installed, the PV system grounding must be harmonized with the requirements specified in National Fire Protection Act (NFPA) 789, Lightning Protection, in addition to NFPA 70.

4. National Electrical Safety Code, ANSI CL-1981

The National Electrical Safety Code applies to equipment and conductors in electricity supply stations and to transmission and distribution systems external to the premises wiring covered by ANSI/NFPA-70. It covers the requirements for clearance distances between overhead power distribution conductors and earth, walkways, buildings, etc. It may limit the selection of locations for PV arrays where overhead power conductors have been or are to be installed in the vicinity.

B. REQUIREMENTS NOT SPECIFIED BY CODE

1. Electrical Interference Control

Another requirement for grounding (other than the need to limit touch voltage[2] and to ensure prompt interruption of ground faults) is control of conducted and radiated electrical noise over a broad frequency range. Switching transistors and their controls in PV power conditioning units can be sources of electrical noise. Also, external sources of noise can interfere with the normal operation of solid-state switching elements in the conditioner, which converts the solar photovoltaic array's dc output to ac.

At this time it does not appear that the Federal Communication Commission (FCC) regulations that limit line-conducted and radiated electrical interference have been defined specifically for solar photovoltaic systems. However, because these systems are intended to be installed in residential as well as in commercial areas, the FCC's more restrictive "B" limits would be expected to be applied. Application of these restrictions to solar photovoltaic systems would be a compelling reason for designers of these systems to incorporate good grounding and shields in their designs.

Proposed Article 690-61, Loss of Utility Voltage, specifies that the power from a utility intractive power conditioning unit shall be automatically disconnected from all ungrounded conductors of the utility system upon loss of voltage in the utility system and shall not reconnect until the utility voltage is restored. If line voltage is required to commutate the power conditioner's inverter, this requirement would be satisfied except for voltage pulses or noise that may be present or occur during a power interruption.

---

[2]The voltage that can occur between any two accessible conducting surfaces.

Even when utility line voltage is present, spurious voltage impulses and electrical noise can interfere with the proper switching of solid-state power devices and operation of their controls. Grounded conductors, enclosures, and shields are frequently used to establish and maintain a set of "zero signal reference conductors" within the system that are essential to the control of unwanted electrical noise and impulses.

Grounding conductor lengths, routing, sequence of ground interconnections, and the location of terminating points can affect ground conductor impedance and the effectiveness of shielding at radio frequencies. Where control of electrical noise is important, code requirements for safety usually permit some alternatives in the manner in which the grounding is accomplished so that the installation can be safe and effective in noise control.

2. Control of dc Injection into the ac System

Article 690 does not address possible problems that could be created by dc and substantial harmonic current injected into the ac system. Such problems could result from specific designs that depend upon matched component characteristics or from component failure.

Possible overheating of transformers and interruption of power are not as serious a safety hazard as electrical shock or interference with ground-fault interruption. However, this issue will more likely become a UL standard requirement rather than a future requirement of the National Electrical Code.

C. IMPLICATIONS UPON PV INTERCONNECTION REQUIREMENTS

The safety and grounding requirements described in subsections A-1 and A-2 appear to cover essential safety requirements without imposing unreasonable design requirements or prohibiting a transformerless system.

System grounding requirements in the proposed Article 690-41 state that: "For a photovoltaic power source, one conductor of a two-wire system and a neutral conductor of a three-wire system shall be solidly grounded." It also permits one exception: "Other methods which accomplish equivalent system protection and which utilize equipment listed and identified for the use."

After referring to the definitions, it seems clear that this requirement is intended to apply to one of the dc output conductors of the PV array. The conducting parts of the PV array frame should be grounded via electrically continuous conduit and/or an equipment ground conductor to the conditioner and to the ground system of the ac utility circuits. The PV array frame and the conduit may also be deliberately or accidentally connected to other ground conductors or grounded pipes and structural members at multiple waypoints.

These grounding requirements can result in a transformerless conditioner being connected to ground at its dc input and through an ac output to a grounded utility power circuit. This could result in a ground loop being formed with current flowing through two connections to ground (driven earth rods, building structural steel, or other qualified ground connection). A bonding conductor between the two ground points would assure that a dangerous voltage would not develop between them, but if the bonding conductor carried some of the PV array's dc output current, some of it would pass through the parallel ground loop path and could create unwanted corrosion damage to structural steel, pipes, and driven ground electrodes.

Article 690-42, Point of System Grounding Connection, permits the dc grounding connection to be made at any single point on the photovoltaic output circuit. For lightning protection, this connection to ground should be as close to the array as possible; however, to prevent unwanted ground loop currents it may be necessary to ground the array's dc output to a ground conductor that has a direct path to the first upstream utility power source ground.

If the PV array's dc output conductor grounding point is located at some distance from the array, a lightning arrestor or controlled gap could be placed at the array. In the event lightning or a high-voltage surge should cause the arrestor or gap to conduct, causing a momentary local low impedance path to ground, the magnitude of the surge that would otherwise flow through the conditioner may be reduced, and the lightning arrestor would restore the system to a single-point ground after the event.

The conducting frame of the photovoltaic array is normally connected via electrically continuous conduits, equipment ground, or both. Grounding, then, can be accomplished by using a common grounding point or separate grounds that have been bonded together, as recommended in Article 690-44, Common Grounding Electrode.

Finally, unless a single-phase, 125-V connection is to be made to the utility, no ground fault indicators are required.

In complying with or taking permitted exceptions to code requirements, the following basic safety objectives in grounding contained in the National Electrical Code ANSI/NFPA 70 Fine Print Note to Section 250-1 should be observed:

(1) Systems and circuit conductors are grounded to limit voltages due to lightning, line surges, or unintentional contact with higher voltage lines, and to stabilize the voltage to ground during normal operation. Systems and circuit conductors are solidly grounded to facilitate overcurrent operation in case of ground faults.

(2) Conducting materials enclosing electrical conductors or equipment, or forming part of such equipment, are grounded to limit the voltage to ground on these materials and to facilitate overcurrent device operation in case of ground faults.

SECTION IV

GENERIC UTILITY CONNECTIONS

There are two possible means of interconnecting a TPCS to a utility distribution transformer as shown in Figures 4-1 and 4-2. It is clear from the figures that one involves a three-wire connection to the utility (including a current carrying neutral) with a green case ground; the other means is a two-wire connection to the distribution transformer with a green case ground.

For simplicity, the array and power conditioner are shown as black boxes. Further, no control or protection circuits are shown as none of these affect the arguments concerning interconnection that follow.

A. TWO-WIRE UTILITY CONNECTION

The two-wire configuration has been proposed as a cost-effective means of implementing a TPCS system. While it is true that no average value dc is imposed on the distribution transformer, there is concern about local, single-phase loads.

Figure 4-3 shows a typical two-wire connection scheme showing idealized switches and currents. Notice that the current in the top half of the circuit appears as a positive half-sine wave, whereas the bottom circuit appears as a negative half-sine wave. The addition of these two waves ensures a full-sine wave in the primary of the distribution transformer.

A single-phase equivalent of the load, Z_L, and the top half of the bridge appear as Figure 4-4. The current source, I_S, can be represented by a Fourier series expansion for a positive half-wave current:

$$I_S = I \frac{2}{\pi} + \frac{1}{2} \cos \omega_{et} + \sum_{n=2,4,6,\cdots}^{\infty} \frac{2}{\pi(1 - n^2)} \cos n\omega_{et}$$

where I is the peak magnitude of the half-wave current source.

The voltage source, V, is a full-wave sine voltage whose value is one-half of that imposed across the secondary of the transformer.

By the use of superposition, the dc component of voltage placed across the load is:

$$V_{Ldc} = \frac{2I}{\pi} \left[\frac{RR_L}{R + R_L} \right]$$

where R_L is the load resistance and R is the cumulative resistances of the transformer and line.

Thus, if reasonable values of R and R_L occur in the system, a reasonable dc voltage will be imposed upon the load. Furthermore, the current harmonics generated by a PCS of this configuration are reasonably high in either of the legs even if perfect half-wave sine waves are assumed, approximately 9%. While this value will be smaller in the load due to current division, unacceptable harmonics may result in customer loads.

B. THREE-WIRE CONNECTION

An idealized three-wire connection is shown in Figure 4-4 along with idealized currents. The important difference to note in this case is that full sinusoidal currents and voltages will result from this type of configuration. Thus, there is no concern about dc injection of current into or dc voltages imposed across consumer loads.

While it is true that the number of components will be higher for this type of connection scheme, the actual additional cost will be quite low. This fact weighed against the better utilization of customer equipment suggests that the three-wire configuration is a better choice for a TPCS. The remainder of this report, therefore, will look at the various issues related to the three-wire utility connection configuration.

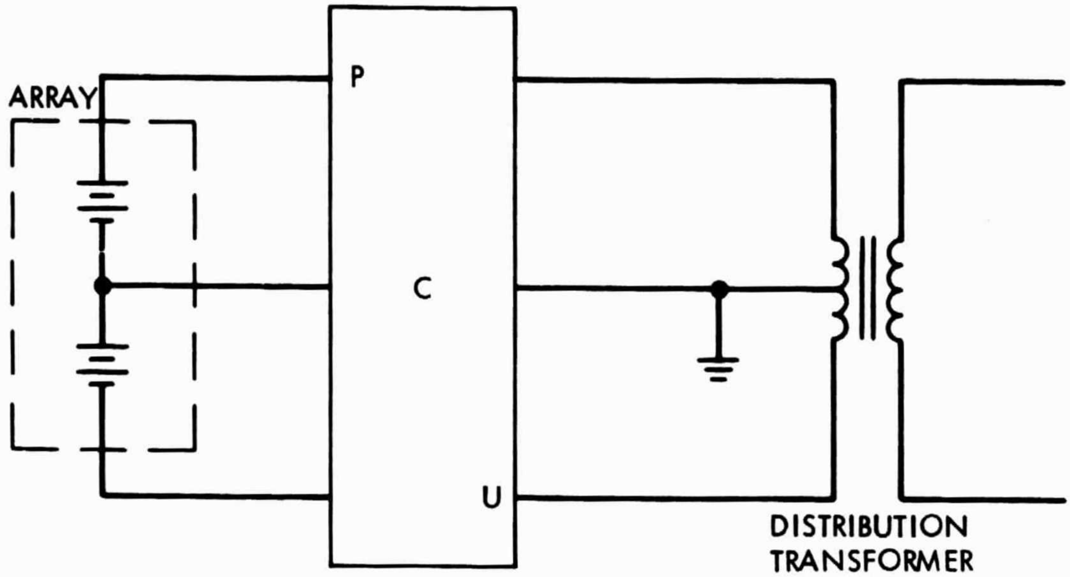

Figure 4-1. Three-Wire Utility Connection

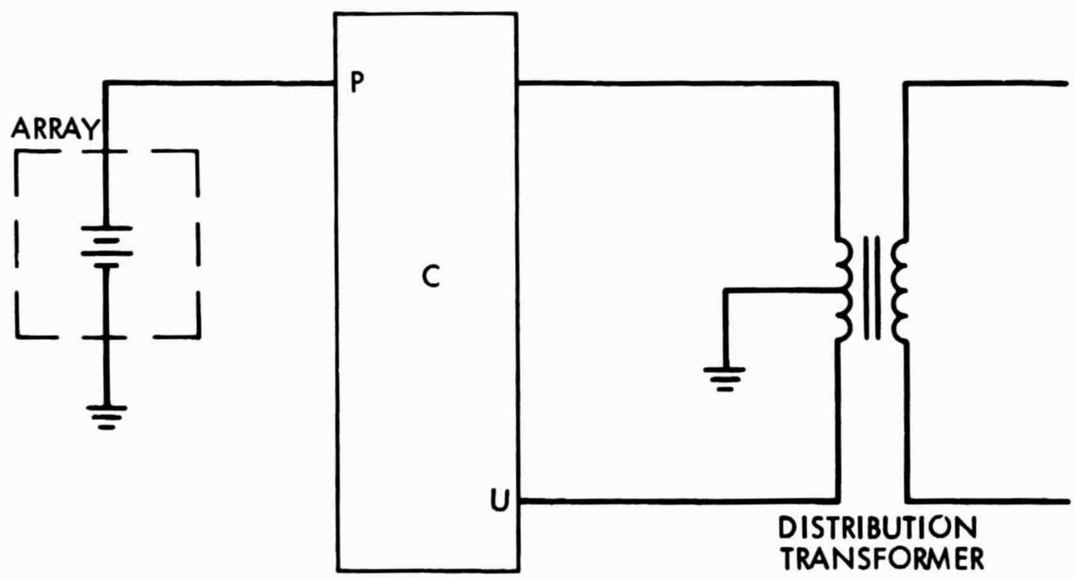

Figure 4-2. Two-Wire Utility Connection

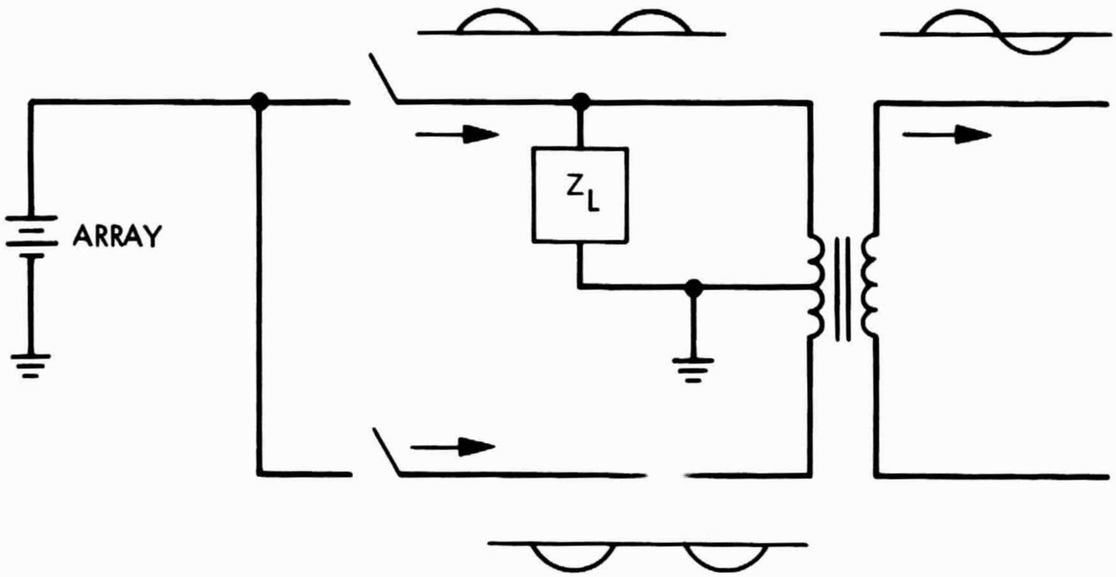

Figure 4-3. Equivalent Circuit Showing Current Waveforms for a Two-Wire Utility Connection

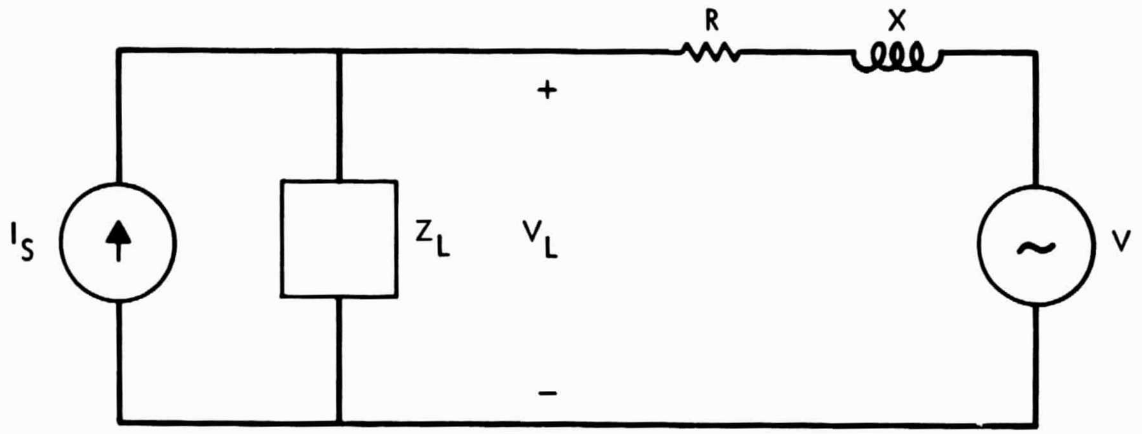

Figure 4-4. Idealized Equivalent Circuit

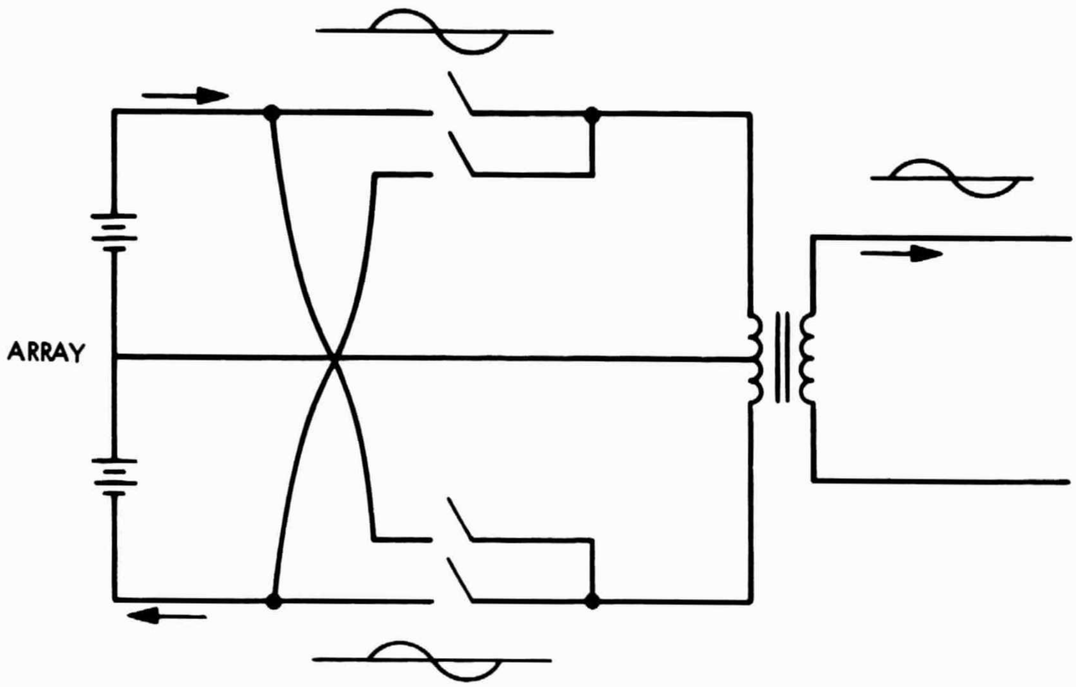

Figure 4-5. Equivalent Circuit Showing Current Waveforms for a Three-Wire Utility Connection

SECTION V

TOPOLOGIES

A. INTRODUCTION

The concerns of both the consumer and utility markets, discussed in Sections III and IV, come to a focal point at the power conditioning subsystem (PCS) where all concerns must be met, either by standard or advanced techniques. One obvious way to meet the concerns for dc injection and isolation is the implementation of an isolation transformer in the PCS design. Another way is to overprotect the system with expensive and sensitive control equipment.

This section presents the results of studies that detail the impacts of three transformerless topologies. The final topology is not really a tranformerless topology but represents the current thinking in advanced PCS topologies, the GE high-frequency link where the transformer is smaller due to the high-frequency preregulator. Of the three transformerless topologies, two are standard bridge circuits and the other is a new design being presented in this report for the first time. Its unique feature is the use of isolating capacitors to ensure negligible dc injection.

Section V is divided into four subsections. The four topologies are presented in some detail with schematics. Next, detailed discussion on sizing is presented for the capacitance and magnetics of each circuit. Finally, the four topologies are compared, based upon the performance criteria of the crossover distortion, component stresses, and failure-mode analysis.

No judgment of the topologies is made in this section. That is reserved for Section VII, where all concerns are brought together in a few recommended topologies.

B. TOPOLOGY DESCRIPTIONS

Four circuit topologies were selected for evaluation as residential inverter candidates. Two of these topologies are voltage-buck circuits in which the solar array voltage must be higher than the peak line voltage. The remaining two topologies have a "boost" capability so that the array potential can be less than the line voltage. All of the topologies employ a modulation technique in which the array voltage is "chopped" into short pulses at a high rate, the pulse widths being altered continuously in such a way that the filtered output closely follows a sinusoidal waveshape. Typically, the carrier frequency is in the range of 10 to 20 kHz, so that there are over 100 cycles of carrier per cycle of 60 Hz.

All the topologies use large filter capacitors across the solar array to reduce the voltage excursions caused by the cyclically varying load current. Also, all the topologies have capacitors across the output of the inverter to reduce the amount of carrier component impressed upon the utility transformer.

Lastly, all the topologies are shown in a push-pull configuration, with the array center-tap connected directly to the utility transformer center-tap and to ground. It should be noted, however, that all calculations in this section have been made on the basis of single-ended systems, i.e., capacitor values should be doubled and inductor values halved.

1. Dual Pre-regulator Bridge

A schematic of a dual pre-regulator bridge is shown in Figure 5-1a. The circuit is composed of a series buck regulator that generates a series of half-sine pulses at a 120-Hz rate, followed by a bridge that inverts alternate half-cycles to match the line-voltage waveform. Transistors Q1-Q2, flyback diodes D1-D2, and inductors L1-L2 form the buck regulator, while transistors Q3-Q6 make up the bridge switch. Capacitors C1-C2 absorb the ac component of input current, while capacitors C3-C4 absorb most of the carrier component of output ripple current. A typical voltage waveform at the input of inductor L1 is shown in Figure 5-2b. The number of carrier pulses has been greatly reduced to show the varying pulse widths.

2. Modulated Bridge

The modulated bridge is shown schematically in Figure 5-2a. The circuit is a buck regulator capable of directly delivering a bi-directional output voltage, so that no separate inverting bridge is required. Transistors Q1-Q4 provide the series switching action required, while diodes D1-D4 provide the flyback function. Inductors L1-L2 control the ripple current fed to output filter capacitors C3-C4. The waveform of Figure 5-2b would be typical of that observed at the upstream (left) end of inductor L1.

3. Cúk Pre-regulator Bridge

Figure 5-3 shows the configuration of a Cúk pre-regulator bridge, which is composed of transistors Q1-Q2, coupling capacitors C5-C6, flyback diodes D1-D2, and inductors L1-L4. The pre-regulator generates half-sine pulses, which are then inverted by bridge switches Q3-Q6, much the same as with the dual pre-regulator bridge circuit described previously. The Cúk circuit has an inverting characteristic, so that input and output are of opposite polarity; this is the reason for the reversal of diodes D1-D2 and transistors Q3-Q6 relative to the dual pre-regulator bridge circuit. Also, inductors L1 and L3 are magnetically coupled, as are L2 and L4. The degree of coupling controls the equivalent source inductance "seen" by the output filter capacitors C3-C4. The ripple current in the output inductors is also strongly affected by the coupling between input and output inductors. The voltage applied to the equivalent output inductance is basically triangular in shape rather than rectangular.

4. General Electric Bridge Pre-Regulator -- Bridge Inverter

The General Electric (GE) bridge pre-regulator, shown in Figure 5-4, is composed of a bridge converter-regulator that generates a series of half-sine pulses, followed by a bridge switch that inverts alternate half-cycles to match the line voltage waveform. The regulating converter is composed of transistors Q1-Q4, step-up interstage transformer T1, bridge rectifier and flyback diodes D1-D4, and filter inductors L1-L2. The bridge switch is composed of SCR1-SCR4. Although functionally similar to the dual pre-regulator bridge, the inclusion of transformer T1 permits the ac line voltage to exceed the array voltage. Inductor input waveforms are similar to those shown in Figure 5-1b.

Table 5-1, showing component parts for each of the four topologies, has been prepared to provide some assistance in estimating the relative complexity of these configurations. Only the major power-handling parts are included. As indicated below, the GE circuit is the most complex, the Ćuk circuit is somewhat less so, and the two buck-regulator circuits are the simplest. The inductors are considered to be single units with dual windings, or, with the Ćuk circuit, four windings.

C. CAPACITOR ESTIMATES

1. Solar Array Filter Capacitor Estimates (C_1, C_2)

The inverter output voltage and current waveforms are essentially sinusoids at a 60-Hz frequency. The power output is thus a "1-cosine" waveform at a 120-Hz frequency. Because the inverter is nominally a lossless device and the input voltage is essentially fixed, the inverter input current also has a "1-cosine" form at 120 Hz. To maximize the use of the solar array power

Table 5-1. Component Count

Component Parts	Dual Pre-Regulator	Modulated Bridge	Ćuk	General Electric
Transistors	6	4	6	4
SCRs				4
Diodes	2	4	2	4
Capacitors	4	4	6	4
Inductors	1	1	1[a]	1
Transformers				1
Total	13	13	15	18

[a]Four rather than two windings.

capability, it is desirable to minimize deviations from the array maximum power point. Some form of filter, usually a large capacitor, is thus needed to absorb the ac component of inverter input current.

If it is assumed that the array absorbs a negligible portion of the inverter input ripple current, the following expression gives a means of estimating the capacitance value, C, required:

$$\frac{\Delta V_1}{V_1} = \frac{P_{av}}{\omega C \; V_1^{\,2}}$$

where

ΔV_1 = peak-to-peak ripple voltage variation

V_1 = input voltage

P_{av} = average power

ω = line angular velocity

C = filter capacitance

For example, for a power level of 4000 W, input voltage of 200 V, angular velocity of 377 rad/s (60 Hz), and a ripple voltage fraction of 0.05, the resulting capacitor size is 5305 μF. A ripple fraction of 0.05 reduces the loss of array power capability to less than 1%. The impedance of the above capacitor is approximately 0.25 Ω at the 120-Hz ripple frequency; because the array dynamic inpedance is about 10 Ω at the maximum power point, only about 2.5% of the ripple current will flow to the array. The RMS current in the capacitor is given by the expression:

$$I = \frac{P_{av}}{V_1\sqrt{2}}$$

where the parameters are as defined above. For the prior example the resulting capacitor current is 14.14 A, RMS.

The above expression for RMS current is only valid for circuits in which the input carrier ripple current is small, such as the Ćuk circuit. For the buck regulator circuits and the GE circuit the filter capacitor RMS currents are affected by duty ratio considerations, and the expression becomes:

$$I = I_p \left[\frac{V_p}{V_1}\left(\frac{4}{3\pi}\right) - \left(\frac{V_p}{V_1}\right)^2 \left(\frac{3}{8}\right) \right]^{1/2} \qquad (5.1)$$

where

I_p = peak output current
V_p = peak output voltage
V_1 = input voltage

for the buck circuits and n times the above for the GE circuit, where n is the transformer turns ratio.

2. Inverter Output Ripple Voltage (C_3, C_4)

The amount of high-frequency (carrier) ripple voltage that the inverter imposes on the utility transformer is of concern because of its EMI potential. Sufficient filtering must be provided in the inverter to ensure that this ripple voltage is reduced to an acceptable level. The output ripple characteristics of the two buck-regulator circuits and the GE circuit are similar; the Cúk circuit differs somewhat.

In the buck regulators the input voltage waveform to the filter inductor is essentially rectangular, with varying dwell times at either the plus input voltage or zero for the dual pre-regulator bridge, or at either the plus or minus input for the modulated bridge. With the GE circuit this voltage is either "n" times the input voltage or zero, "n" being the transformer turns ratio. In any case, the resulting inductor current waveform is nearly triangular. The output filter capacitor absorbs most of this ripple current; the resulting capacitor (and output) voltage is closely approximated by two successive parabolic waveforms of opposite curvature. With these approximations the peak-to-peak output ripple voltage may be calculated as:

$$\Delta v_c = \frac{V\left(1 - \frac{V}{V_1}\right)}{8f^2LC}$$

where

Δv_c = ripple voltage
V = output voltage
V_1 = input voltage
f = carrier frequency
L = inductance value
C = capcitance value

for the dual pre-regulator circuit. For the GE circuit, V_1 is replaced by nV_1. For a fixed input voltage the ripple voltage has a maximum value when the output voltage is half the input voltage, corresponding to a 50% duty ratio. The maximum ripple voltage thus becomes:

$$\Delta v_c = \frac{V_1}{32f^2LC} \tag{5.2}$$

As an example, for a 1% ripple fraction (of V_1)and a 20-kHz frequency, the required LC product is 7.81, with L in millihenries and C in microfarads.

For the modulated bridge circuit the expression for peak-to-peak output ripple voltage is:

$$\Delta v_c = \frac{V_1 \left[1 - \left(\frac{V}{V_1}\right)^2\right]}{16f^2LC}$$

where the parameters are as defined above. In this case the maximum ripple voltage occurs when the output voltage is zero. At this point the maximum ripple voltage is given by:

$$\Delta v_c = \frac{V_1}{16f^2LC} \tag{5.3}$$

Note that twice the LC product is required for this circuit to obtain the same ripple as the pre-regulator bridge.

In the Ćuk circuit the coupling capacitors (C5 and C6 in Figure 5-3) are subjected alternately to the input and output currents; because these currents are nearly constant over a carrier cycle, the resulting capacitor voltage waveform is nearly triangular. This voltage is imposed upon the equivalent output inductance of the Ćuk circuit, causing the inductor current waveform to appear as successive parabolic segments of opposite curvature. The output filter capacitor performs one more integration, so that the capacitor (and output) voltage waveform is a series of linked cubic segments. The expression for peak-to-peak output ripple voltage is given by:

$$\Delta v_{co} = \frac{I}{12f^3LC_cC_o}\left(\frac{V}{V_1 + V}\right)^3$$

where

ΔV_{co} = ripple voltage

I = output current

f = carrier frequency

L = inductance value

C_c = coupling capacitance

C_o = output capacitance

V = output voltage

V_1 = input voltage

The maximum ripple occurs with maximum output for this circuit. As an example, for $I = 25$ A, $f = 20$ kHz, $L = 1$mh, $C_c = 10\,\mu F$, $C_o = 5\,\mu F$, $V = 325$ V, and $V_1 = 200$ V, the peak-to-peak ripple voltage is 1.235 V.

3. Capacitor Charging Currents

One of the considerations in the design of a switching regulator for use with the modulation approach described previously is the extent to which the switching semiconductors are penalized by having to switch the output filter capacitor charging currents as well as the load current. For the Cuk circuit this consideration also applies to the charging currents for the coupling capacitors.

The peak charging current for the buck-regulator output capacitors is given by the following expression:

$$I_{pc} = V_p \omega C$$

where

I_{pc} = peak value of capacitor charging current

V_p = peak line voltage

ω = angular velocity

C = capacitor value

For a nominal line voltage of 230-V RMS and a 60-Hz frequency the peak capacitor charging current is 0.123 A/μF, and it occurs at the line voltage zero crossing. In the buck regulator the semiconductors must switch this current, which, for reasonable sizes of capacitors (10 to 20 μF), amounts to a few amperes. Because the peak charging currents occur at the time of minimum load current, there does not appear to be a need to increase semiconductor size to accommodate capacitor charging currents. The same rationale applies to the GE circuit except that the semiconductor currents are increased by the turns ratio of the interstage transformer. In the Cúk circuit the charging current for the output capacitors is the same as with the buck regulators, but the relation to the semiconductor current is different. In both circuits the capacitor current, I_c, is given by:

$$I_c = V_p \omega C \cos \omega t$$

where t is time and the other parameters are as defined previously. The input current that must be switched by the semiconductors is given by the expression:

$$I_1 = \frac{V_p^2}{V_1} \omega C \sin 2\omega t$$

where

V_1 = input voltage

I_1 = input current

This function reaches a maximum when ωt is 45 deg, the peak value being given by:

$$I_{1p} = \frac{V_p^2}{V_1} \omega C$$

where I_{1p} = peak input current.

For a nominal input voltage of 200 V and a line voltage of 230-V RMS, the peak input current is 0.199 A/μF. Because the peak input for capacitor charging is displaced 45 deg from the peak load current, there does not appear to be a penalty in semiconductor size although the margins are somewhat smaller than with the buck-regulator circuits.

The coupling capacitors for the Cúk circuit also require charging currents to be switched by the semiconductors. The expression obtained for this component of input current is given by:

$$I_{pc} = V_p \omega C \left(1 + \frac{V_p}{V_1} \sin \omega t\right)^2 \cos \omega t \qquad (5.5)$$

where the parameters are as defined previously. This expression reaches a maximum value when the following relation is satisfied:

$$\sin \omega t = -\frac{V_1}{6V_p} + \left[\left(\frac{V_1}{6V_p}\right)^2 + \frac{2}{3}\right]^{1/2} \tag{5.6}$$

For an input voltage of 200 V and an RMS line voltage of 230 V the maximum occurs at ωt = 46.1 deg, giving a peak input current for charging the coupling capacitors of 0.252 A/μF. Although the angle for the maximum value of peak charging current increases with a decreasing ratio of V_1/V_p, the function approaches a limit at about 55 deg, which is sufficiently separated from the 90-deg load peak to ensure that the coupling capacitor charging currents do not add significantly to the semiconductor switching requirements.

D. MAGNETICS

1. Design Equations for Magnetic Components

Design equations have been developed for performing preliminary estimates of the characteristics of the magnetic components (transformers and inductors) that are the major mass contributors to each of the four topologies investigated. The equations are general in form and lead to both mass and power loss estimates. The examples given are those that represent the extremes of the operating conditions and thus tend to maximize the size of the magnetic components.

a. Transformer (General Electric Design). The current-handling capability of a transformer is directly dependent upon the cross-sectional area of the core window as this determines the total number of ampere turns available. The core cross-sectional area, correspondingly, is directly related to the voltage developed per turn for a given flux density and frequency of operation. The product of these two areas is therefore a good indication of the power handling capability of the transformer. These factors have been combined into the following equation:

$$A_p = \frac{N_v N_w P_p}{4fk_w B_m J_m} \tag{5.7}$$

where

- A_p = core/window area product
- P_p = peak power capability
- f = frequency of operation
- B_m = peak flux density
- J_m = peak current density
- k_w = window utilization factor

The parameter, N_v, is a coefficient whose value depends on whether the load current continues to flow through the transformer during the transistor "off" (flyback) period or ceases at the end of the duty cycle. The answer to this question depends upon the implementation of the controls for the transistor bridge; if the conducting transistors are switched off simultaneously, the flyback current in the transformer is quickly terminated. If sequential switching is employed to reduce transistor switching losses, the flyback current will continue through the transformer. In the latter case the value of N_v is unity. In the former instance N_v is determined from:

$$N_v = \left(\frac{8\ V_p}{3\pi n V_1}\right)^{1/2}$$

where

- V_p = peak output voltage
- n = turns ratio
- V_1 = input voltage

As an example, for an input voltage of 200 V, peak ac voltage of 325 V, and a turns ratio of 2, the value of Nv is 0.83.

The parameter, N_w, is a coefficient whose value depends upon whether the primary and/or secondary windings are center-tapped. The following list is the range of values for N_w:

(1)	Plain primary, plain secondary	2
(2)	Center-tapped primary, plain secondary	$1+\sqrt{2}$
(3)	Plain primary, center-tapped secondary	$1+\sqrt{2}$
(4)	Center-tapped primary, center-tapped secondary	$2+\sqrt{2}$

Both N_v and N_w are related to heating effects in the windings.

As an example of use of the equation for area product, using a value of 1 for N_v, a value of 2 for N_w, and assuming a peak power of 8000 W, frequency of 10 kHz, window utilization factor of 0.4, peak flux density of 0.6 Teslas and peak current density of 500 A/cm^2 (500×10^4 A/m^2), the calculated value of area product is 33.3×10^{-8} m^4, or 33.3 cm^4.

b. <u>Inductor (Single Winding for Pre-regulator Bridge and GE Design)</u>. The design equations for the inductors are similar in form to those developed for the transformer. The only additional parameter is F_m, the maximum allowable ripple current fraction. This parameter is defined as the ratio of the maximum peak-to-peak ripple current to peak value of output current. One of the main considerations in the inductor design is the low frequency (60-Hz) component of flux density, for which an air gap must be provided to prevent core saturation. This analysis assumes that all of the magnetomotive force is absorbed in the air gap, a valid assumption for initial designs. The total flux density, B_T, includes both the low- and high-frequency components; it is analogous to B_m in the transformer design equation. The expression for the area product required is given by:

$$A_p = \frac{P_p}{2fk_w B_T J_m} \left(\frac{V_1}{2F_m V_p} + 1 - \frac{V_p}{V_1} \right) \qquad (5.8)$$

where

A_p = area product

P_p = peak power

f = frequency

k_w = window utilization factor

B_T = peak total flux density

J_m = peak current density

V_1 = input voltage

V_p = peak output voltage

F_m = maximum ripple fraction

The first term in the parenthesis reflects the low-frequency effects and is the dominant term. The last two terms include the high-frequency contribution at the peak of the 60-Hz wave; these terms disappear when the peak output voltage exactly matches the input voltage (100% duty ratio is implied).

As an example, assume a peak power of 8000 W, a frequency of 20 kHz, a window utilization factor of 0.4, a peak total flux density of 1.5 Teslas, a peak current density of 500×10^4 A/m^2, an input voltage of 442 V, a peak output voltage of 311 V, and a maximum ripple fraction of 0.2. The resulting area product is 25.66×10^{-8} m^4, or 25.66 cm^4.

c. Inductor (for Modulated Bridge). The modulated bridge circuit subjects the filter inductor to somewhat different operating conditions than the pre-regulator bridge circuit. The maximum ripple current occurs at zero 60-Hz output rather than at half the input voltage, and the ripple voltage applied to the inductor input is twice as large. The equation describing the required area product is as follows:

$$A_p = \left(\frac{P_p \left(\frac{V_1}{V_p} \right)}{2fk_w B_T J_m} \right) \left[\frac{1}{F_m} + 1 - \left(\frac{V_p}{V_1} \right)^2 \right] \tag{5.9}$$

where the parameters are as defined previously. This equation is valid for ripple fractions up to 0.5, which should include nearly all cases. Using the values indicated in the previous example, the calculated area product is 52.16 cm^4. Note that the inductor is about twice the size of the inductor for the dual pre-regulator and GE circuits.

d. Inductor (For Cúk Circuit). The inductor design for the Cúk circuit is different from the transformer and buck-regulator inductor designs in two ways: (1) The currents in the two windings on the Cúk inductor are not related by the turns ratio and (2) They have different waveshapes and therefore different ratios of peak current to RMS current. In spite of this, the equation for area product is not radically different from the previous design equations. The area product is given by:

$$A_p = \frac{N_y P_p}{fk_w B_T J_m} \left(\frac{N_x}{F_m} + \frac{1}{2} \right) \left(\frac{\frac{V_p}{V_1}}{1 + \frac{V_p}{V_1}} \right) \tag{5.10}$$

where

P_p = peak power

f = frequency

k_w = window utilization fact

B_T = peak total flux density

J_m = peak current density

F_m = maximum ripple fraction

V_p = peak output voltage

V_1 = input voltage

The parameter, N_y, arises from heating considerations for the input and output findings. The expression for N_y is:

$$N_y = \sqrt{\frac{2}{\pi}} + n \frac{V_1}{V_p} \tag{5.11}$$

where n = turns ratio.

For example, with a turns ratio of 1.4, an input voltage of 225 V, and a peak output voltage of 311 V, the value of N_y is 1.811.

The parameter, N_x, reflects the relative contributions of the two windings to the low-frequency component of flux density. The expression for N_x is:

$$N_x = 1 + n \frac{V_1}{V_p} \tag{5.12}$$

with parameters defined previously.

N_x and N_y would have identical expressions except that the input current waveshape has a "1-cosine" form rather than a half-sine form and therefore a lower ratio of RMS to peak current. Using the parameter values given in the example for N_y, the value of N_x is 2.013.

Using the above values for N_x, N_y, V_1 and V_p, and assuming a peak power of 8000 W, a frequency of 20 kHz, a window utilization factor of 0.4, a peak total flux density of 1.5 Teslas, a peak current density of 500×10^4 A/m^2, and a maximum ripple fraction of 0.2, the calculated area product, A_p, for the Cuk circuit inductor is 148×10^{-8} m^4, or 148 cm^4.

Note that the inductor for the Ćuk circuit is much larger than the inductor for the dual pre-regulator inverter. There are three major factors that are responsible for this difference:

(1) There are two windings with roughly equal ampere-turns, which require about twice the core window area.

(2) The two windings have cumulative ampere-turns, which requires about twice the core area and air gap to avoid core saturation.

(3) In the Ćuk circuit the maximum ripple current occurs at the peak output and therefore contributes heavily to the peak design constraints, while in the dual pre-regulator system, the maximum ripple occurs at roughly half of peak output and the contribution at peak output is small.

2. Magnetic Component Mass

To make mass estimates for the magnetic components involved in the four topologies, the generalized core configuration shown in Figure 5-5 was used as an analysis tool. In this Figure, A is the lamination width, B is the stack height, C is the window width, and D is the window length. The windings are located on the left and right end legs of the core. For the Cuk inductor a smaller center leg is also involved whose lamination width is rA. Only a single gap is shown for each core leg although two would probably be used in actual practice. Using these parameters, the expression for the net core volume is:

$$\text{Core Volume} = k_s AB\,[2C + (2 + r)(D + 2A)]$$

where k_s is the core stacking factor, and r is zero for all but the Cuk inductor. Correspondingly, the net winding volume is:

$$\text{Winding Volume} = k_w\, CD[2(A + B) + \frac{\pi}{2} C]$$

where k_w is the window utilization factor. The area product is given by:

$$\text{Area Product} = ABCD$$

By assuming a constant core geometry so that

$$\frac{B}{A} = k_{ab},\ \frac{D}{C} = k_{cd},\ \text{and}\ \frac{CD}{AB} = k_{wc}$$

these equations may be rewritten in the form:

$$\text{Core Volume} = k_s A^3 k_{ab}\left[2\sqrt{\frac{k_{ab}k_{wc}}{k_{cd}}} + (2 + r)\left(\sqrt{k_{ab}k_{cd}k_{wc}} + 2\right)\right] \quad (5.13)$$

$$\text{Winding Volume} = k_w A^3 k_{ab} k_{wc}\left[2(1 + k_{ab}) + \frac{\pi}{2}\sqrt{\frac{k_{ab}k_{wc}}{k_{cd}}}\right] \quad (5.14)$$

$$\text{Area Product} = A^4 k_{ab}^2 k_{wc} \quad (5.15)$$

Once the geometry constants k_{ab}, k_{cd}, k_{wc} and r have been selected, the value of A can be found by using Equation (5.15) and the required area product. Core and winding volumes can then be found by using this value in Equations (5.13) and (5.14). Core and winding masses may then be obtained by multiplying the volumes by the appropriate densities.

Although these equations (5.13, 5.14, and 5.15) can be used to estimate absolute masses of alternative magnetic options, a rough comparison can be made by assuming identical geometries and noting that the mass is proportional to A^3 while the area product is proportional to A^4. Mass is thus proportional to area product raised to the three-quarters power. Using the previous examples of 25.66 cm^4 for a dual pre-regulator inductor and 148 cm^4 for the Cúk circuit inductor, the implied mass ratio is $(148/25.66)^{3/4}$, 3.72.

Using the foregoing examples of required area product, applying the more rigorous equations (5.13, 5.14, and 5.15) and assuming that $k_{ab} = 1.0$, $k_{ed} = 2.0$, $k_{wc} = 2.5$ and $r = 0.4$ for the Cúk inductor, the core and winding volumes and masses of the inductors and the GE transformer have been calculated and are shown in Table 5-2. In all cases the window utilization factor, k_w, is assumed to be 0.4, and the core stacking factor, k_s, is 0.92. Core and winding densities assumed are 8.2 g/cm^3 and 8.96/cm^3, respectively.

3. Magnetic Component Losses

The losses in magnetic components are composed of winding loss and core loss. If the RMS current densities in the windings are uniform, the winding loss can be expressed:

$$\text{Winding Loss} = \rho \frac{J_m^2}{2} (\text{Vol}) \tag{5.16}$$

Table 5-2. Core and Winding Volumes and Masses for Inductors and GE Transformer

Core Volumes and Winding Masses	Dual Pre-Regulator	Modulated Bridge	Cúk	General Electric Inductor	General Electric Transformer
Core volume, cm^3	56.5	96.1	243.3	56.5	68.64
Winding volume, cm^3	33.0	56.2	122.7	33.6	40.11
Core mass, kg	0.463	0.788	1.995	0.463	0.563
Winding mass, kg	0.296	0.503	1.099	0.296	0.359
Total mass, kg	0.758	1.291	3.094	0.759	0.922

where

ρ = winding resistivity
J_m = peak current density
Vol = winding volume

The peak current density, J_m, rather than RMS density has been used in Equation (5.16) to be consistent with other equations used in the analyses.

Core loss can be expressed in the general form:

$$\text{Core Loss} = k_L f^x B^y,$$

where

k_L = a constant dependent on core material and lamination thickness

f = frequency

B = peak ac flux density

x and y = empirical constants dependent on core material and lamination thickness

When a rectangular voltage waveform is modulated by a sine wave, as is the case with all of the topologies being investigated in this report, the expression for core loss becomes more complex:

$$\text{Core Loss} = k_L f^x \frac{2}{\pi} \int_0^{\frac{\pi}{2}} \left(B\ (\theta)\right)^y d\theta \qquad (5.17)$$

where B is now of function of θ, the phase angle. Because the exponents x and y are usually decimals, the expression cannot be integrated in closed form, and integration must be done by a computer.

The expression for $B(\theta)$ for the GE transformer is:

$$B(\theta) = \frac{N_v N_w P_p \sin\theta}{4fk_w A_p J_m} \qquad (5.18)$$

where

P_p = peak power
f = frequency
k_w = window utilization factor
A_p = area product
J_m = peak current density
N_v and N_w = winding usage coefficients defined in Section 5.4.1

The expression for $B(\theta)$ for the inductors is dependent upon the type of regulator circuit. For the dual pre-regulator the expression is:

$$B(\theta) = \frac{P_p \sin\theta \left(1 - \frac{V_p}{V_1} \sin\theta\right)}{2fk_w A_p J_m} \qquad (5.19)$$

where

P_p = peak power
V_p = peak output voltage
V_1 = input voltage
f = frequency
k_w = window utilization factor
A_p = area product
J_m = peak current density

For the GE inductor, V_1 must be replaced by n V_1, where n is the transformer turns ratio.

For the modulated bridge circuit the expression for ac flux density has the following form:

$$B(\theta) = \frac{P_p \frac{V_p}{V_1} \left[1 - \left(\frac{V_p}{V_1} \sin\theta\right)^2\right]}{4fk_W A_p J_m} \qquad (5.20)$$

where the parameters are as defined for Equation (5.19).

The Cúk circuit has a somewhat different expression:

$$B(\theta) = \frac{N_y P_m}{2fk_w A_p J_m} \left[\frac{\frac{V_p}{V_1} \sin\theta}{1 + \frac{V_p}{V_1} \sin\theta}\right] \qquad (5.21)$$

where

$$N_y = \sqrt{\frac{2}{\pi}} + n \frac{V_1}{V_p} \tag{5.22}$$

and n = inductor turns ratio.

Core losses were computed for all inductors and the GE transformer, using the extreme values of array and line voltages (high array voltage and low line voltage) for design levels, but with nominal operating values. The core material assumed for all inductors was a 2-mil, 3% silicon steel. The core material for the transformer was assumed to be a 2-mil, 50% nickel-iron alloy. Peak flux densities for all inductors were 1.5 Teslas; the transformer was assumed to operate with a peak flux density of 0.6 Teslas. The computed core losses in Watts per kilogram are given in the first line of the following table.

Using the above values for core loss per kilogram and the core mass estimates made in the previous section, an estimate was made of the actual core loss. Also, using the previous expression for winding loss and assuming a peak current density of 500 A/cm^2 and a resistivity for copper of 1.67 micro-ohm-cm, the winding losses were calculated (Table 5-3).

As indicated previously, the Cúk inductor, which is considerably larger than the buck inductor, has a much greater power loss. Also, considering the relatively large core loss in the transformer, it probably would have been better to assume an 80% nickel-iron alloy with lower losses per kilogram even though the mass would be greater.

Table 5-3. Losses for the Four Topologies

Losses	Dual Pre-Regulator	Modulated Bridge	Cúk	General Electric Inductor	General Electric Transformer
Core, W/kg	25.47	34.17	15.74	25.47	65.77
Core, W	11.79	26.93	31.40	11.79	37.02
Winding, W	6.89	11.73	25.61	6.89	8.37
Total, W	18.68	38.66	57.01	18.68	45.39

E. SEMICONDUCTOR LOSSES

Semiconductor losses are primarily composed of conduction and switching losses. Conduction losses in a transistor used in switching applications are a result of the collector-omitter voltage drop with the transistor in a saturated condition. This voltage drop can be modeled quite well by a small fixed voltage in series with a resistor. Similarly, a diode voltage drop can also be modeled by a fixed voltage and a series resistance; the fixed voltage is typically much higher in a diode than in a transistor.

Representative component models in the range of interest are given in the following sketch.

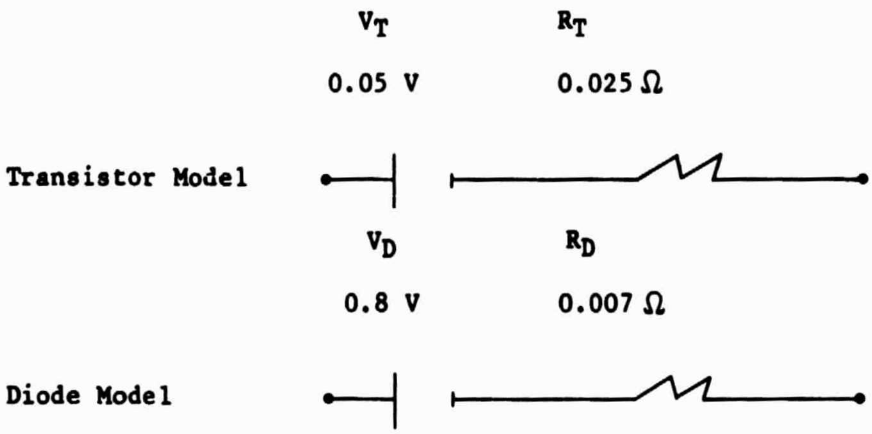

Using these models and equations describing the inverter voltage, as well as current and duty ratio variations with phase angle, the average power losses in the semiconductors have been calculated.

For the dual pre-regulator bridge and the modulated bridge circuits the conduction loss in the regulator transistors is:

$$\text{Loss} = \frac{P_p}{V_1}\left(\frac{V_T}{2} + \frac{4}{3} R_T \frac{P_p}{V_p}\right) \qquad (5.23)$$

where

P_p = peak power
V_1 = input voltage
V_p = peak output voltage
V_T and R_T = as described in the previous sketch

For a peak power of 8000 W, a nominal input voltage of 398 V and a peak line voltage of 325 V, the calculated transistor conduction loss is 5.75 W per transistor.

The conduction loss in the flyback diodes is given by the following expression:

$$\text{Loss} = \left[\frac{P_p}{V_p} V_D\left(\frac{2}{\pi} - \frac{1}{2}\frac{V_p}{V_1}\right) + R_D\frac{P_p}{V_p}\left(\frac{1}{2} - \frac{4}{3}\frac{V_p}{V_1}\right)\right] \tag{5.24}$$

The calculated diode loss for the conditions in Equation (5.24) is 5.15 W per diode.

For the Cúk circuit the transistor conduction loss is given by:

$$\text{Loss} = \frac{2}{\pi}\frac{V_p P_p}{V_1^2}\int_o^{\frac{\pi}{2}}\left(\frac{V_T \sin^3\theta + R_T\frac{P_p}{V_1}\sin^5\theta}{1 + \frac{V_p}{V_1}\sin\theta}\right)d\theta \tag{5.25}$$

where the parameters are previously defined. The corresponding flyback diode loss is given by:

$$\text{Loss} = \frac{2}{\pi}\frac{P_p}{V_p}\int_o^{\frac{\pi}{2}}\left(\frac{V_D \sin\theta + R_D\frac{P_p}{V_p}\sin^2\theta}{1 + \frac{V_p}{V_1}\sin\theta}\right)d\theta \tag{5.26}$$

The indicated integrations were performed on a computer, resulting in a calculated transistor loss of 9.60 W (each) and a diode loss of 6.65 W (each) for a peak power of 8000 W, a peak line voltage of 325 V and an input voltage of 200 V. As might be expected, the conduction losses for the input transistors are apppreciably higher for the Cúk circuit because the input voltage is lower and the currents are correspondingly higher.

Output bridge conduction losses were estimated in a similar manner. The output bridge has a duty ratio of one, which simplifies the calculation. The expression obtained is:

$$\text{Loss} = \frac{P_p}{V_p}\left(\frac{2}{\pi}V_T + \frac{R_T P_p}{2V_p}\right) \tag{5.27}$$

where the parameters have been defined previously. Using the above expression and the values given in Equation (5.26), the calculated total output bridge loss for the dual pre-regulator bridge and the Cúk circuits is 16.72 W. For the GE circuit, which uses SCRs in the output bridge, the transister and diode models were combined to form an SCR model. The resulting total output bridge loss was 46.02 W.

Estimates of transistor switching losses have been made for the several inverter circuits. For each switching operation the transistor collector voltage must rise or fall through a voltage, V_{ce}, while the collector current must fall or rise through a range, I_c. In general, with the inductive load line presented by the filter inductor, the transistor must carry the full collector current while the collector voltage is changing, resulting in a triangular loss waveshape. Therefore, the average power loss over one carrier cycle is:

$$\text{Loss} = V_{ce} I_c f(T_r + T_f)$$

where

f = carrier frequency

T_r = rise time

T_f = fall time

By describing V_{ce} and I_c in terms of the circuit voltages and currents, the average collector loss can be found by integrating the resulting expression over one-quarter cycle of the 60-Hz waveform. The resulting expression for the dual pre-regulator bridge is:

$$P_c = \frac{V_1 P_p f\,(T_r + T_f)}{\pi V_p} \qquad (5.28)$$

where

P_c = collector switching loss (total)

P_p = peak power

V_p = peak line voltage

f, T_r, and T_f = (see definitions above)

As an example, for a nominal input voltage of 398 V, a peak power of 8000 W, a frequency of 20 kHz, rise and fall times of 0.5 μs, and a peak line voltage of 325 V, the calculated switching loss is 62.4 W.

In the modulated bridge circuit the collector voltage swing is twice as great as the dual pre-regulator bridge because the flyback diode allows the emitter voltage to become negative (array voltage) rather than zero (common). Under nominal conditions the switching loss is thus 124.8 W.

For the Ćuk circuit the total switching loss is:

$$P_c = P_p f (T_r + T_f) \left(\frac{1}{4} + \frac{2V_p}{3V_1} \right) \tag{5.29}$$

where the parameters are as defined previously for Equation (5.28). The calculated switching loss with a 200-V input, other parameters having the above values, is 95.2 W. Table 5-4 is a compilation of the semiconductor losses.

Switching losses have been neglected for the GE circuit, based on the assumption that the commutating capacitors contained therein can reduce the switching losses to a negligible value. As can be noted from Table 5-4, switching losses can be a significant part of the semiconductor losses.

F. PERFORMANCE COMPARISON

1. Crossover Distortion

There is an inherent waveform distortion product created by those circuits employing a pre-regulator to generate a series of unidirectional

Table 5-4. Semiconductor Losses for Four Topologies under Study

	Conduction Loss			
Models	Dual Pre-Regulator	Modulated Bridge	Ćuk Circuit	General Electric Circuit
Input transistors	10.50	10.50	19.20	43.78
Diodes	10.30	10.30	13.30	29.32
Output bridge	16.72	--	16.72	46.02
Total loss	37.52	20.80	49.22	77.02
	Switching Loss			
	Dual Pre-Regulator	Modulated Bridge	Ćuk Circuit	General Electric Circuit
Input transistors	62.4	124.8	95.2	--
Total loss	99.92	145.60	144.42	77.02

half-sine pulses and a bridge switch to invert alternate half-sine pulses to match the utility waveform. The modulated bridge does not have a pre-regulator and as such has no crossover distortion. Figures 5-6 through 5-8 show this characteristic. The desired inductor current waveform has the half-sine shape shown in Figure 5-6, in which the peak value is about 25 A for a 4-kW system. This is basically the load current waveform, neglecting the effects of the output filter capacitor. Neglecting the resistance of the inductor, the voltage across the inductor to produce the desired current waveform is shown in Figure 5-7, in which the peak value is about 9.5 V/mH for a peak current of 25 A. When added to the half-sine load voltage, the voltage needed upstream of the filter inductor has the shape shown in Figure 5-8. Unfortunately, the pre-regulator cannot deliver a negative voltage, so the inductor current cannot be driven to zero in time to start the rise of the next half-sine pulse. This results in distortion of the output waveform in the vicinity of the zero crossover.

A greatly expanded view of the crossover region is given in Figure 5-9, in which the sine wave segments have been replaced by their tangents. V_1 and V_2 are the voltages upstream and downstream of the filter inductor. The angle θ is the phase angle between V_1 and V_2, as defined by the equation:

$$\sin \theta = \frac{\omega LP}{V_1 V_2}$$

where

ω = angular velocity

L = inductance value

P = power

V_1 = upstream voltage

V_2 = downstream voltage

For a power flow of 4000 W, a frequency of 60 Hz, and V_1 and V_2 values of 230 V, the angle θ is approximately 1.63 deg/mH, corresponding to about 75 μs/mH.

An expanded view of the inductor current is given in Figure 5-10, in which the ideal current follows the straight line with a negative slope down to intersect the time axis at the point labeled θ/ω. At this time the bridge switch is reversed, and the ideal current rises along the line with the positive slope. The actual inductor current will deviate from the ideal at zero time and will tend to follow the parabolic path until it becomes tangent to the rising straight line through the origin, at which time the bridge is switched and the current rises along this line. The displacement of the actual current from the ideal will inject excess current into the output filter capacitor until the excess is bled off into the utility transformer.

The excess charge represents an error voltage across the filter capacitor; the approximate shape of the error voltage is shown in Figure 5-11. The first portion of this curve is a cubic resulting from the parabolic current error; after the bridge switch is reversed at θ/ω, the curve is a straight line. This curve is based on the assumption that the utility transformer drains away a negligible portion of the excess charge, which is probably valid for the first few hundred microseconds, depending upon the transformer reactance. Note that the error voltage is very sensitive to the inductor size; the functional relationship is cubic.

Some reduction in the distortion could be achieved by holding the voltage V_1 at zero for a period of about $2\theta/\omega$ and then releasing V_1 to its original path and switching the bridge at this time. This action is indicated by the dotted lines in Figure 5-9. The corresponding current waveform is indicated by the lower parabolic curve in Figure 5-10. Note that the current curve returns to the ideal with zero steady-state error.

2. Component Voltage and Current Stresses

There are three main factors that affect the evaluation of inverter component stresses: the range of line voltages, the variation of solar array voltage with temperature, and the ratio of array open circuit voltage (V_{oc}) to the maximum power-point voltage (V_{mp}). For the following analyses the ac line voltage was assumed to vary from 220 to 250 V RMS, the array temperature range was assumed to be 0 to 50°C with a temperature coefficient of -0.5%/°C, and the V_{oc}/V_{mp} ratio was estimated to be 1.25. Although this temperature range may not be the worst-case extreme, it should be broad enough to be indicative of the temperature effects on the component stresses.

It was assumed that the inverter must be capable of delivering full power (4000 W) to the utility over the full range of array and utility voltage variations. The combination of low array voltage and high line voltage establishes the minimum array voltage for the voltage buck inverters (Figures 5-1 and 5-2) and the transformer turns ratio for the GE design (Figure 5-4). It is assumed in this case that the regulator duty ratio can reach 100%; if this is not valid, some additional margin must be left for duty ratio limitations. Also, it was assumed that the inverter must be capable of generating at very light loads so that the array voltage could approach its open circuit value.

The maximum voltage stresses occur with the combination of high line voltage and maximum array voltage. Table 5-5 is a listing of the peak component voltages for the several inverter designs and the equations from which these values were derived. The quantities V_{mp} and V_{oc} are as defined before; V_p is the peak ac line voltage (to the nearest volt) corresponding to 250 V RMS, and n is the transformer turns ratio for the GE design. The modulator bridge design places the highest voltage stress on its transistors, in fact, the level indicated may be prohibitively high. The GE circuit has the highest diode voltage stress although the level shown may be acceptable for selected diode types.

Current stresses are generally at their maximums for the conditions of low array and line voltages. Table 5-6 shows the current stresses for the components listed in the previous table except for the output filter capacitors (C_3 and C_4), which in all cases are only carrying a relatively small ripple current. Peak currents were calculated for all semiconductors because of their importance to this study. RMS currents were calculated for capacitors because heating is the primary consideration. One new parameter, the peak power (P_p), is indicated in the table; the remaining parameters have been defined previously. Except where footnoted, the equations that determine the amount of current are given in Table 5-6. As might be expected, the buck inverter designs have the lowest current stress.

Current stress estimates were also made for the magnetic elements of the four designs, the results of which are shown in Table 5-7. The new parameters are average power, P_{av}, and RMS line voltage, V_{rms}. Because heating effects are of primary concern, the currents calculated are RMS values.

The general approach used to calculate RMS currents, where the current waveform is a square pulse, pulse-width modulated by the 60-Hz sinusoid, was to calculate the RMS current value of an arbitrary carrier pulse and integrate the square of the resulting expression over a quarter-cycle to obtain the overall RMS value. For each carrier cycle it is assumed that the current is constant at one value during the transistor "on" time and constant at another value during the transistor "off" time.

3. Failure-Mode Effects

Failure modes, both open and short circuit, have been considered for each of the capacitors and semiconductors in each of the four topologies being evaluated. The qualitative effects of each of these failures have been estimated, and the results are given in Tables 5-8 through 5-11. A review of these tables indicate that many of the failures are potentially catastrophic in their effects and that the inverter must be quickly disconnected from the utility. In some cases continued operation may be possible in a degraded mode, usually at reduced power output. All of the topologies are vulnerable to failures in their output components, especially the capacitors and bridge semiconductors; there is no great advantage of one topology over another in this regard.

Table 5-5. Component Peak Voltage Stress

Inverter Designs/Components		Peak Voltage, V
Dual Pre-Regulator (V_{mp} = 442, V_{oc} = 552, V_p = 354)		
C_1-C_2	$V_{oc}/2$	276
Q_1-Q_2	$V_{oc}/2$	276
D_1-D_2	$V_{oc}/2$	276
Q_3-Q_6	V_p	354
C_3-C_4	$V_p/2$	177
Modulated Bridge (V_{mp} = 442, V_{oc} = 552, V_p = 354)		
C_1-C_2	$V_{oc}/2$	276
Q_1-Q_4	V_{oc}	552
D_1-D_4	V_{oc}	552
C_3-C_4	$V_p/2$	177
Ćuk Circuit (V_{mp} = 225, V_{oc} = 281, V_p = 354)		
C_1-C_2	$V_{oc}/2$	141
Q_1-Q_2	$(V_{oc}+V_p)/2$	318
C_5-C_6	$(V_{oc}+V_p)/2$	318
D_1-D_2	$V_p/2$	177
Q_3-Q_6	V_p	354
C_3-C_4	$V_p/2$	177
General Electric Circuit (V_{mp} = 225, V_{oc} = 281, V_p = 354, n = 2.02)		
C_1-C_2	$V_{oc}/2$	141
Q_1-Q_4	V_{oc}	281
D_1-D_4	nV_{oc}	568
SCRI-SCR_4	V_p	354
C_3-C_4	$V_p/2$	177

Table 5-6. Component Current Stress

Inverter Designs/Components		Peak Current, A
<u>Dual Pre-Regulator</u> (V_p = 311, P_p = 8000, V_{mp} = 442)		
C_1-C_2 RMS	(a)	8.64
Q_1-Q_2 Peak	P_p/V_p	25.72
D_1-D_2 Peak	P_p/V_p	25.72
Q_3-Q_6 Peak	P_p/V_p	25.72
<u>Modulated Bridge</u> (V_p = 311, P_p = 8000, V_{mp} = 442)		
C_1-C_2 RMS	(a)	8.64
Q_1-Q_4 peak	P_p/V_p	25.72
D_1-D_4 peak	P_p/V_p	25.72
<u>Ćuk Circuit</u> (V_p = 311, P_p = 8000, V_{mp} = 175)		
C_1-C_2 RMS	$P_p/(2\sqrt{2}\,V_{mp})$	16.16
Q_1-Q_2 Peak	P_p/V_{mp}	45.71
C_5-C_6 RMS	(2)	22.34
D_1-D_2 Peak	P_p/V_p	25.72
Q_3-Q_6 Peak	P_p/V_p	25.72
<u>General Electric Circuit</u> (V_p = 311, P_p = 8000, V_{mp} = 175, n = 2.02)		
C_1-C_2 RMS	(b)	17.46
Q_1-Q_4 Peak	$n(P_p/V_p)$	51.96
D_1-D_4 Peak	P_p/V_p	25.72
SCR_1-SCR_4 Peak	P_p/V_p	25.72

(a)

$$I = \left[\frac{P_p}{V_p}\,\frac{V_p}{V_{mp}}\left(\frac{4}{3\pi}\right) - \left(\frac{V_p}{V_{mp}}\right)^2\left(\frac{3}{8}\right)\right]^{1/2}$$

(b)

$$I = n\,\frac{P_p}{V_p}\left[\frac{V_p}{V_{mp}}\left(\frac{4}{3\pi}\right) - \left(\frac{V_p}{V_{mp}}\right)^2\left(\frac{3}{8}\right)\right]^{1/2}$$

Table 5-7. Magnetic Element RMS Current Stress

Inverter Designs/Components		Peak Current, A
Dual Pre-Regulator (P_{av} = 4000, V_{rms} = 220)		
L_1-L_2	P_{av}/V_{rms}	18.18
Modulated Bridge (P_{av} = 4000, V_{rms} = 220)		
L_1-L_2	P_{av}/V_{rms}	18.18
Ćuk Circuit (P_{av} = 4000, V_{rms} = 220, V_{mp} = 175)		
L_1-L_2	$(3/2)^{1/2}\ P_{av}/V_{mp}$	27.99
L_3-L_4	P_{av}/V_{rms}	18.18
General Circuit (P_{av} = 4000, V_{rms} = 220, V_p = 311, P_p = 8000, V_{mp} = 175, n = 2.02)		
L_1-L_2	P_{av}/V_{rms}	18.18
T_1 Sec. (I_s)	$(2P_p/V_p)\ (V_p/3\pi n V_{mp})^{1/2}$	15.71
T_1 Pri.	$n(I_s)$	31.73

Table 5-8. Component Failure Mode Effects for Dual Pre-regulator Bridge

Fault	Effect
C_1 or C_2 Short	Pre-regulator and/or bridge transistors subjected to reverse polarity collector voltages. Probable semiconductor breakdown and fault imposed on utility transformer
C_1 or C_2 Open	Large array voltage swing with loss of filtering action, possibly causing reverse potentials on semiconductors with subsequent failure and imposition of array voltages on the utility transformer
Q_1 or Q_2 Short	Imposition of array voltage on utility transformer, resulting in large dc currents and probable saturation of the utility transformer
Q_1 or Q_2 Open	Half-sine pulses fed to alternate halves of the utility transformer on alternate half-cycles. This is a possible survival mode, although at reduced power output
D_1 or D_2 Short	Reverse potentials applied to bridge transistors, with probable subsequent failure and overload of utility transformer
D_1 or D_2 Open	Loss of commutation, causing large transient voltages to appear across pre-regulator transistors, probably resulting in failure of one of these components and imposition of array voltage on utility transformer
Q_3-Q_6 Short	Direct short on utility transformer on alternate half-cycles, resulting in saturation
Q_3-Q_6 Open	Unbalanced power flow through the utility transformer on alternate half-cycle will tend to force the transformer into partial saturation, possibly enough to cause transformer fuses to blow
C_3 or C_4 Short	Direct short on utility transformer, causing main circuit breaker to the PV installation to open
C_3 or C_4 Open	Excessive high-frequency ripple voltage applied to utility transformer, possibly causing EMI problems

Table 5-9. Component Failure Mode Effects for Modulated Bridge

Fault	Effect
C_1 or C_2 Short	Bridge transistors subjected to reverse voltages, with probable failure and shorting of utility transformer
C_1 or C_2 Open	Large array voltage swing with loss of filtering action, possibly causing reverse potentials on bridge semiconductors with subsequent failure and imposition of array voltages on the utility transformer
Q_1-Q_2 Short	Direct coupling of the array and its filter capacitor to the utility transformer, probably saturating the transformer and rupturing the array filter capacitor
Q_1-Q_4 Open	Asymmetrical drive to the utility transformer on alternate line half-cycles will tend to force the transformer into partial saturation, possibly causing transformer fuses to blow
D_1-D_4 Short	Direct coupling of the array and its filter capacitor to the utility transformer, probably saturating the transformer and destroying the filter capacitor
D_1-D_4 Open	Loss at commutation, causing large transient voltages to appear across bridge transistors, probably causing a transistor failure and coupling the array directly to the utility transformer
C_3 or C_4 Short	Direct short on utility transformer, causing fuses to blow
C_3 or C_4 Open	Excessive high-frequency ripple voltage applied to utility transformer, possibly causing EMI problems

Table 5-10. Component Failure Modes Effects for Cúk Pre-Regulator Bridge

Fault	Effect
C_1 or C_2 Short	Half-sine pulses fed to alternate halves of the utility transformer on alternate half-cycles. This is a possible survival mode, but with reduced power capability
C_1 or C_2 Open	Large array voltage swing with loss of filtering action. Power capability would be reduced and distorted current waveforms fed to utility transformer
Q_1 or Q_2 Short	Reverse potentials applied to bridge transistors through coupling capacitors, possibly causing transistor breakdown and shorting of the utility transformer
Q_1 or Q_2 Open	Half-sine pulses applied to alternate halves of the utility transformer on alternate half-cycles. This is a possible survival mode, but with reduced power capability
C_5 or C_6 Short	Reverse potentials applied to bridge transistors, probably causing transistor breakdown and shorting of the utility transformer
C_5 or C_6 Open	Half-sine pulses applied to alternate halves of utility transformer on alternate half-cycles. This is a possible survival mode at reduced power
D_1 or D_2 Short	Reverse potentials applied to bridge transistors, probably causing transistor breakdown and shorting of the utility transformer
D_1 or D_2 Open	Loss of commutation, causing large transient voltages to appear across pre-regulator, probably causing transistor failure, which in turn may cause failure of the bridge transistors and a short on the utility transformer
Q_3–Q_6 Short	Direct short on utility transformer on alternate half-cycles, resulting in overload and saturation
Q_3–Q_6 Open	Asymmetrical drive to the utility transformer on alternate line half-cycles will tend to force the transformer into partial saturation, possibly causing transformer fuses to blow
C_3 or C_4 Short	Direct short on utility transformer, causing fuses to blow
C_3 or C_4 Open	Excessive high-frequency ripple voltage applied to utility transformer, possibly causing EMI problems

Table 5-11. Component Failure Mode Effects for GE High-frequency Bridge

Fault	Effect
C_1 or C_2 Short	Greatly reduced power output and probable distortion in current waveform because of limited (half-normal) array voltage
C_1 or C_2 Open	Large array voltage swing with loss of filtering action. Reduced power capability and probable current waveform distortion. Possible survival mode
Q_1-Q_4 Short	Direct short in interstage transformer on alternate carrier half-cycles, resulting in saturation and distorted waveform applied to bridge rectifiers. Some portion of this distortion passed on to utility transformer
Q_1-Q_4 Open	Interstage transformer driven into saturation by asymmetric drive. Some portion of distorted output waveform passed through bridge rectifier to utility transformer
D_1-D_4 Short	Direct short on interstage transformer output on alternate carrier half-cycles. Some portion of distorted output fed to utility transformer through SCR bridge
D_1-D_4 Open	Interstage transformer driven into saturation by asymmetric load current. Distorted output fed to utility transformer through SCR bridge
SCR_1-SCR_4 Short	Direct short on utility transformer on alternate line half-cycles, resulting in overload and saturation
SCR_1-SCR_4 Open	Unbalanced power flow through the utility transformer on alternate half cycles will tend to force the transformer into partial saturation, possibly blowing the transformer fuses
C_3 or C_4 Short	Direct short on utility transformer, causing fuses to blow
C_3 or C_4 Open	Excessive high-frequency ripple voltage applied to utility transformer, possibly causing EMI problems

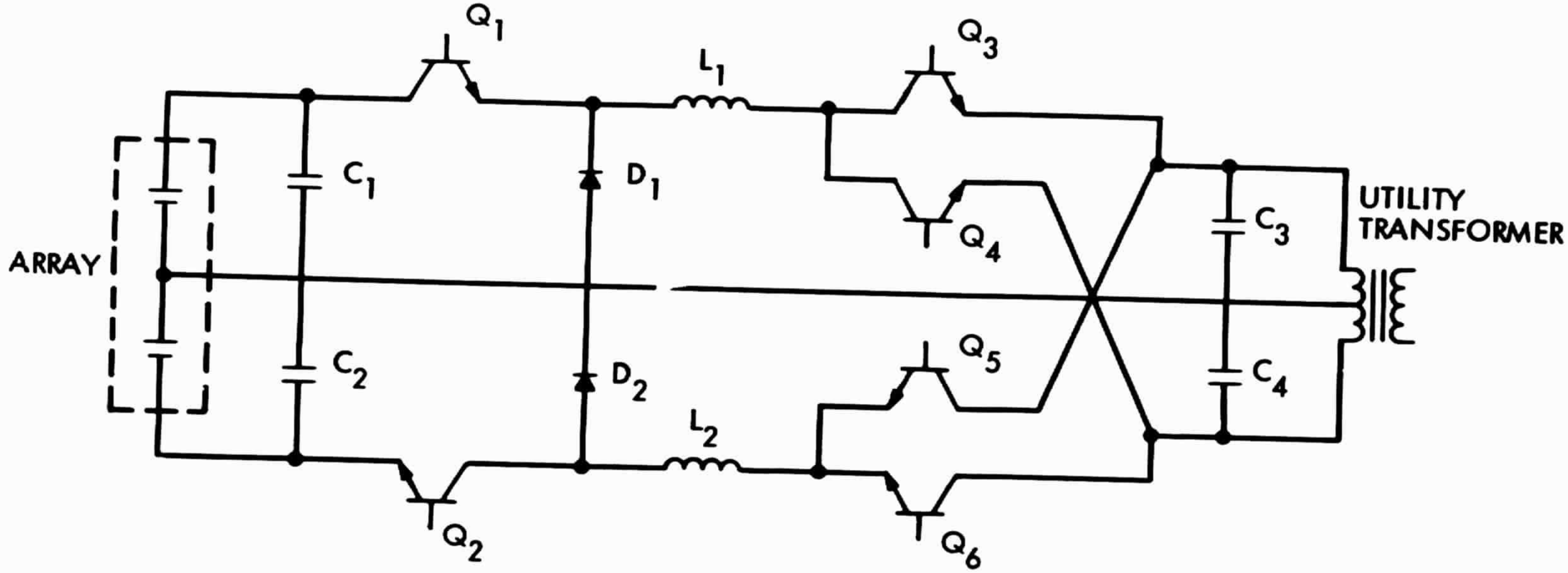

Figure 5-1a. Dual Pre-regulator Bridge

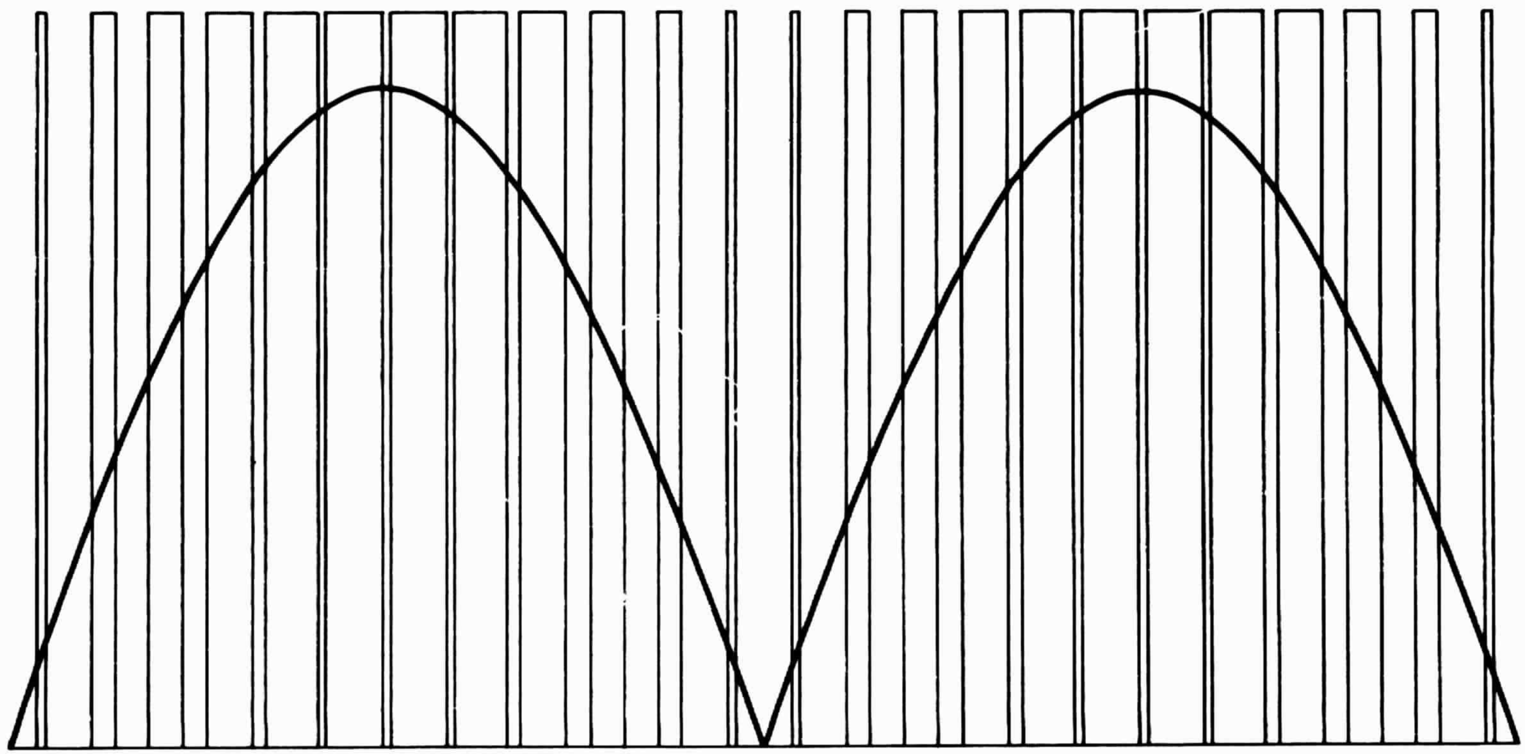

Figure 5-1b. L_1 Input Waveform for Pre-regulator Bridge

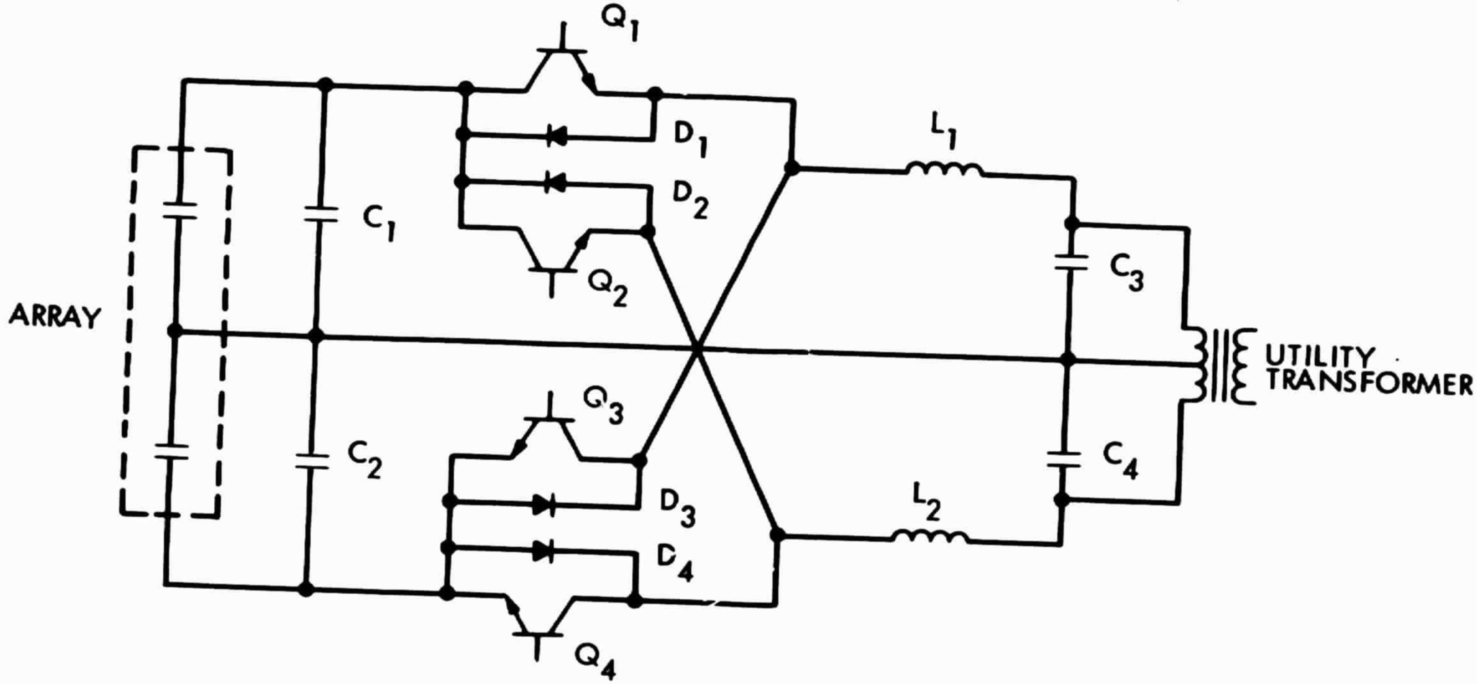

Figure 5-2a. Modulated Bridge

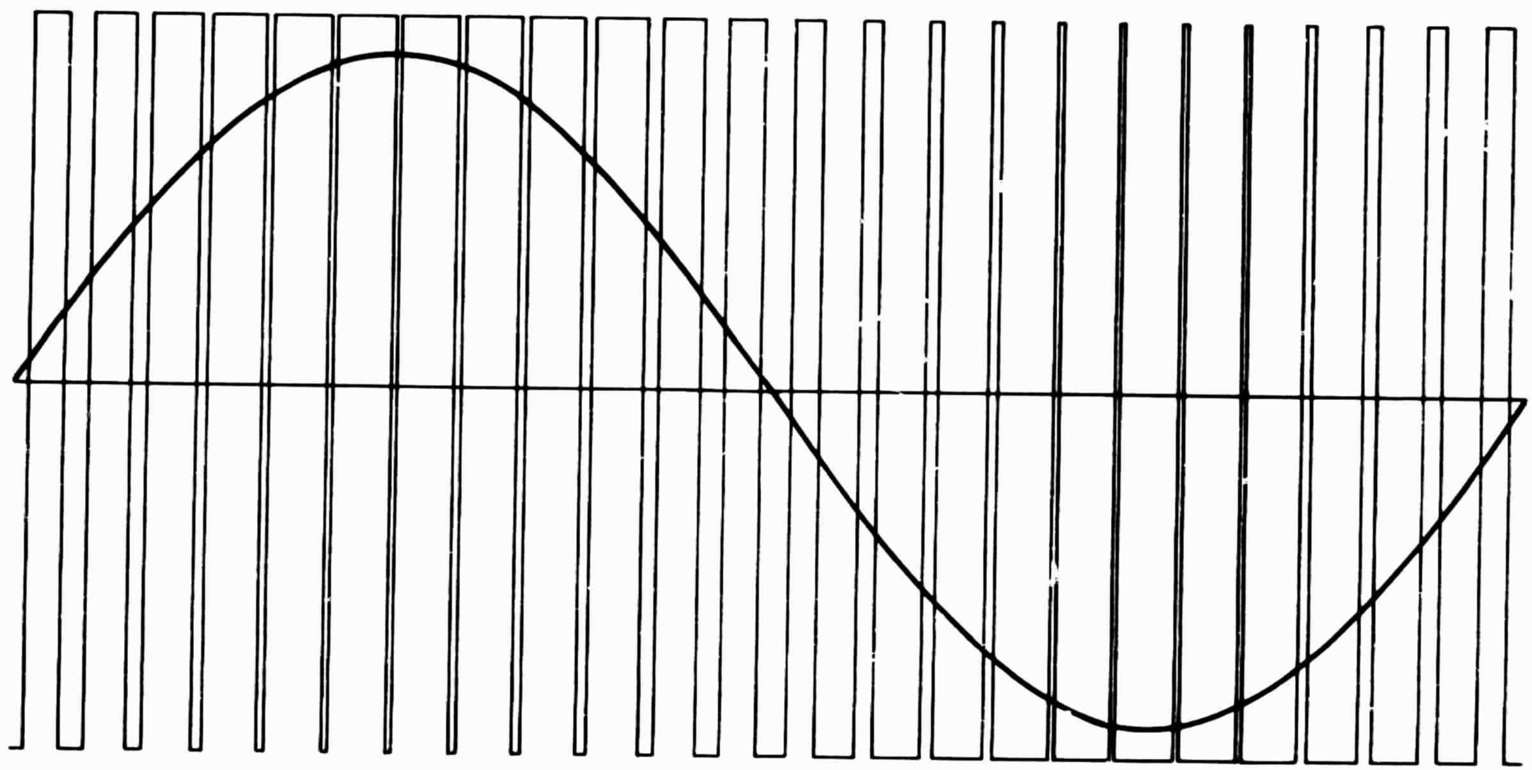

Figure 5-2b. L_1 Input Waveform for Modulated Bridge

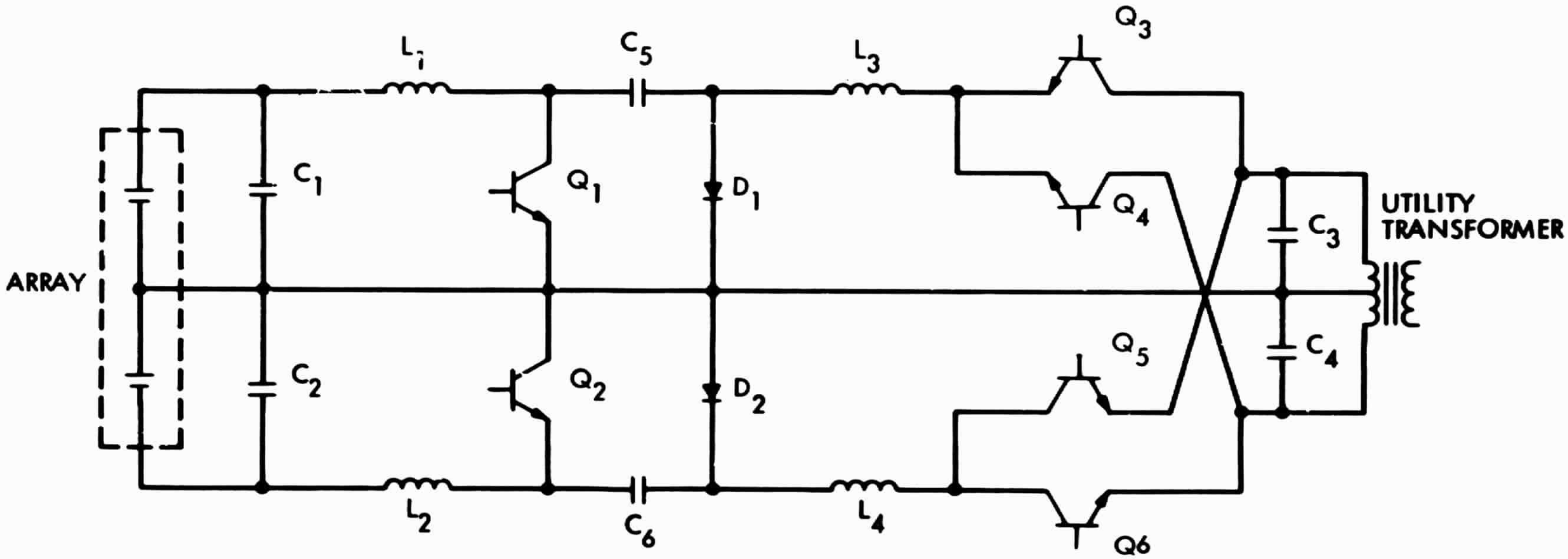

Figure 5-3. Ćuk Pre-regulator Bridge

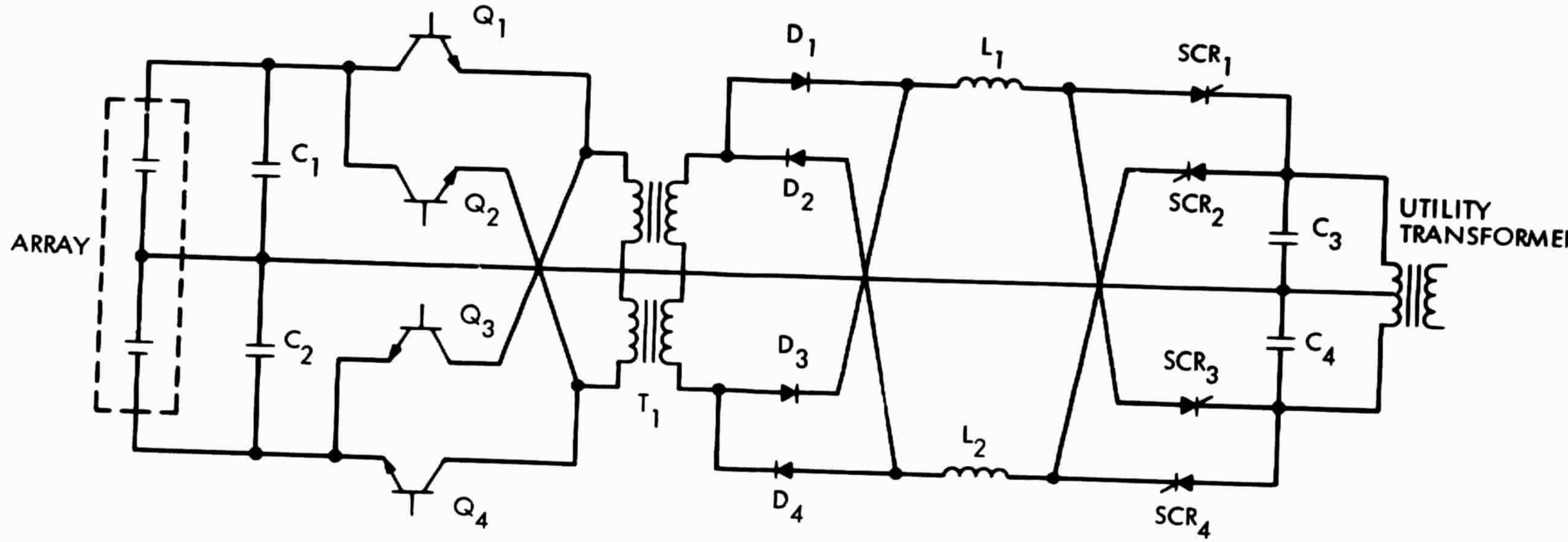

Figure 5-4. General Electric Bridge Pre-regulator

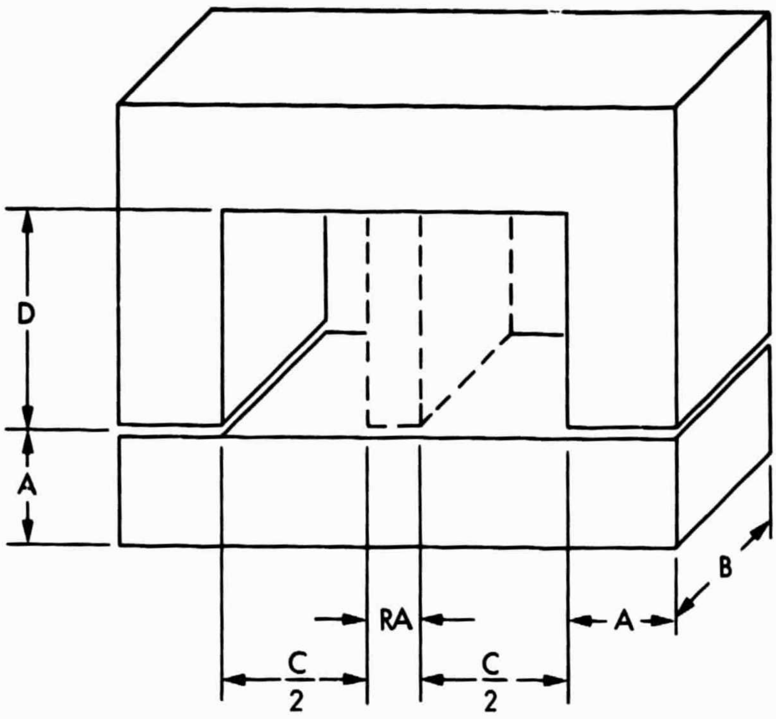

Figure 5-5. General Core Configuration

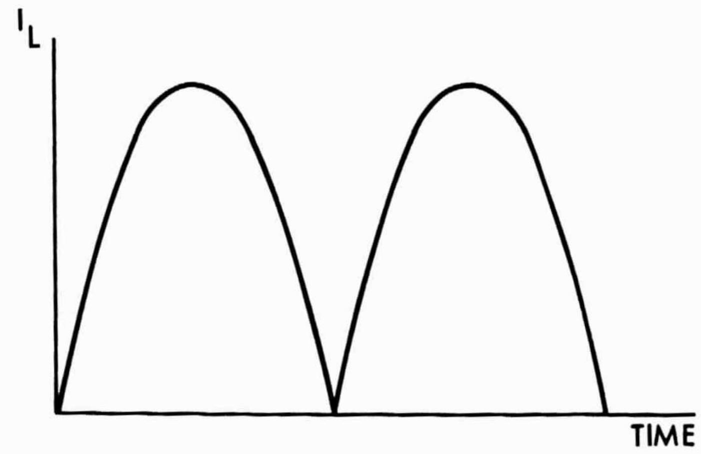

Figure 5-6. Desired Inductor Current Waveform

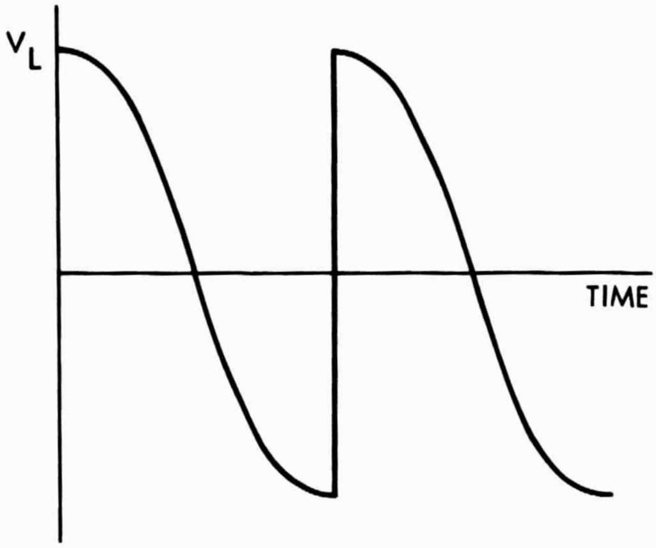

Figure 5-7. Required Voltage Across Inductor

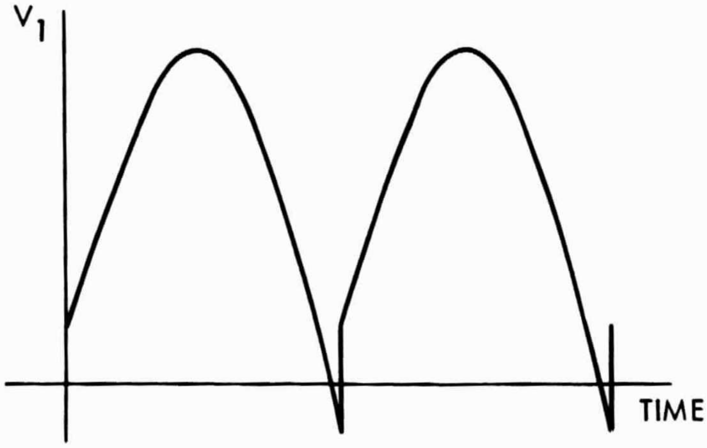

Figure 5-8. Desired Upstream Voltage

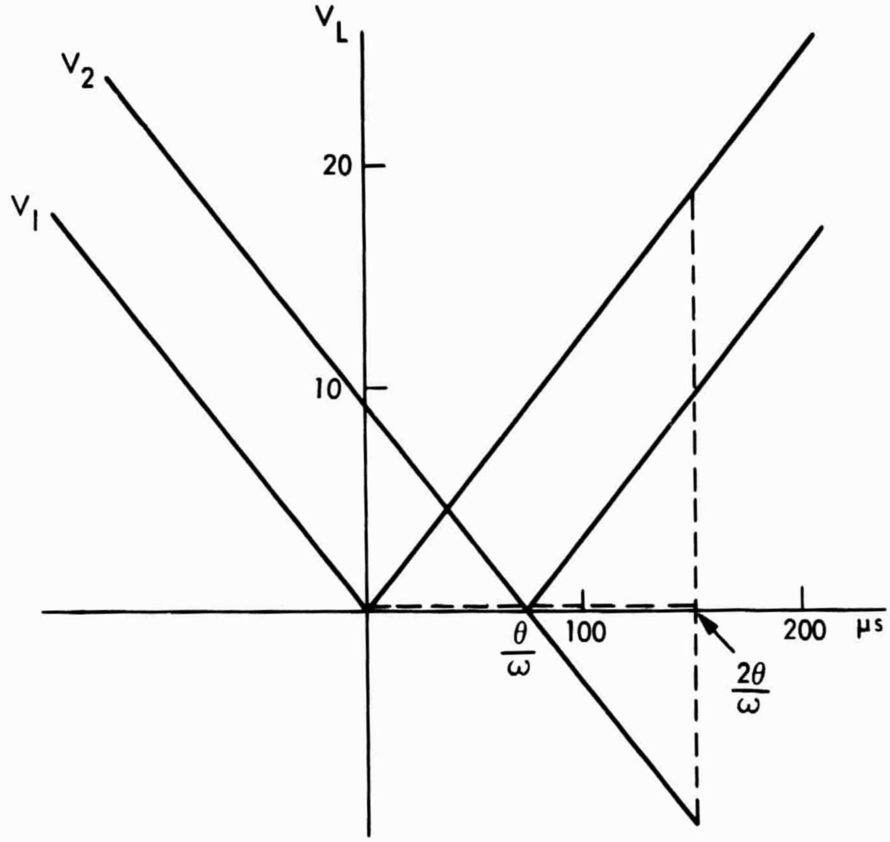

Figure 5-9. Expanded View of Crossover Region

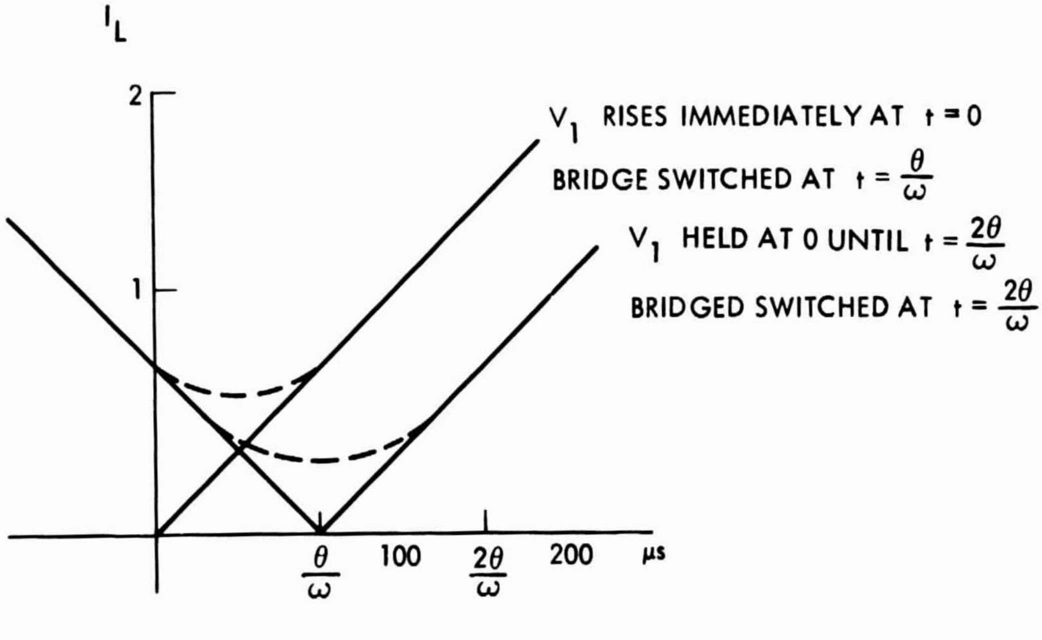

Figure 5-10. Actual Crossover Region

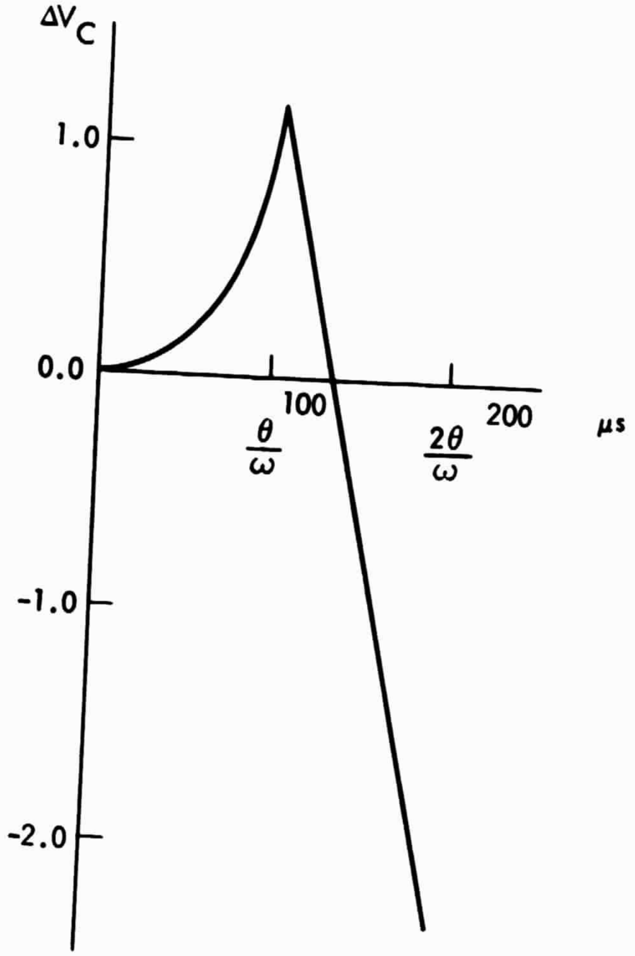

Figure 5-11. Error Voltage Across Capacitor

SECTION VI

DIRECT CURRENT INJECTION

As stated in Section II, prolonged dc injection is to be avoided so that transformer saturation does not occur. Following core saturation, the increased primary current can cause the fused cut-out to open, thus causing a loss of customer service. If more than one customer is on the same distribution transformer, a loss of service will be incurred through no fault of the customer or the utility.

Similarly, if dc current is injected into the power supplies of household equipment (TVs, computers, stereos, etc.) fuses, circuit breakers, or components will fail. If component failure occurs, costly repair bills may be incurred by the owner of a PV system or his immediate neighbors. Initial analysis has shown that the transformers used in these power supplies will not saturate because the load impedance is much larger than the impedance to the system. Therefore, very little dc current will actually flow into the loads, causing equipment malfunction.

This section, therefore, addresses the issue of dc injection into the utility distribution transformer by developing analytical expressions for the time to saturation under a specific operating condition and the steady-state currents that flow following saturation. The results of these expressions show that the time to saturation is on the order of cycles, and following this, the time to fuse failure is tens of seconds under heavily loaded conditions.

A. TIME TO SATURATION

The circuit of concern is shown in Figure 6-1. At time $t = 0$, a step increase in dc current is injected into the secondary of the transformer. The voltage across the primary is:

$$V = L \frac{dI'_{dc}}{dt} + R\, I'_{dc} \qquad (6.1)$$

where I'_{dc} is the injected dc current referred to the primary.

To determine the time to saturation, the amount of accumulated volt-seconds is required. Replacing the integral with its rectangular equivalent Equation (6.1) becomes:

$$\int V dt = L\, I'_{dc} + R\, I'_{dc}\, \Delta t = I'_{dc}\, (L + R\Delta t) \qquad (6.2)$$

Let V be the RMS primary voltage with a corresponding peak core flux of B_o. The volt-seconds associated with B_o becomes:

$$V'dt = \sqrt{2}\, V_1 \quad \frac{2T}{\pi 4} = \frac{V_1}{\sqrt{2\pi f}} \tag{6.3}$$

where the integral is taken over 1/4 cycle and f is 60 Hz.

Thus, the change in flux B that occurs following the injection of dc current is:

$$\Delta B = \frac{B_o \int V dt}{V'dt} = \frac{\sqrt{2}\, \pi B_o f\, I'_{dc}}{V_1} (L + R\Delta t) \tag{6.4}$$

If the transformer is normally operating at B_o, the time to reach saturated conditions B_{sat} (see Figure 6-2) is:

$$\Delta B_o = B_{sat} - B_o$$

$$\Delta B_o = \frac{\sqrt{2}\, \pi B_o f\, I'_{dc}}{V_1} (L + R\Delta t)$$

$$\Delta B_o = \frac{267.31\, I'_{dc}\, B_o}{V_1} (L + R\Delta t) \tag{6.5}$$

Expressing in per unit quantities R' and X':

$$\frac{\Delta B_o}{B_o} = \frac{I'_{dc} V_1}{P} \left[\sqrt{2}\, X' + \frac{2\pi 60}{\sqrt{2}} R'\Delta t\right]$$

$$= \frac{I'_{dc} V_1}{P} \left[0.707\, X' + 267.31\, R'\Delta t\right] \tag{6.6}$$

where P is the power rating of the transformer.

Solving for Δt:

$$\Delta t = \frac{\gamma}{267.31\ R'\lambda} - \frac{2.65 \times 10^{-3}\ X'}{R'} \qquad (6.7)$$

where

$\gamma = \frac{\Delta B_o}{B_o}$ (headroom to saturation)

$\lambda = \frac{I_{dc} V_1}{P}$ ("per unit" dc power)

X' = per unit reactance

R' = per unit resistance

Choosing typical values for R' and X' (0.02 and 0.05, respectively), the family of curves of Figure 6-3 results. Most utilities load their distribution transformers so that a 30% saturation margin occurs (i.e., $\gamma = 0.30$). The results indicate that with very little dc injection, 5% of the ac current, the time to saturation is about 1.1 s (66 cycles). In the other extreme, if the transformer is the same size as the PV array and the entire power is passed as dc into the transformer, the time to saturation is 0.05 s (3 cycles).

An approximate rule of thumb for transformers is that about one-third of the magnetizing current level can occur in the form of dc current. From an analysis of small transformers this implies a value of λ in the range of 0.01 to 0.05. Figure 6-4 shows the time to saturation for low values of λ. In this case, a great deal of time is available to sense the dc current and begin correction procedures before saturation occurs.

B. STEADY-STATE PRIMARY CURRENT

Following the application of a specified dc current, a transient condition occurs, followed by a steady-state condition where the primary current is a function of the operating condition.

During the time when the transformer is not saturated, a current of $I'_{dc} = I_{dc}/n$ (see Figure 6-1) will flow through R and L. The voltage drop across R is R I'_{dc} and across L is zero. This voltage drop will cause the core flux to drift so that saturation will occur once each half cycle (Figure 6-5). When saturation occurs, the source voltage will drop across R and X. For simplification, X is assumed zero (this yields conservative rather than optimistic results.)

As noted in the figure, the positive half-cycle is truncated due to core saturation. The "missing" volt-seconds will equal the volt seconds during the rest of the half-cycle. Approximating the missing segment (shaded area of Figure 6-5) by a triangle of height V_p and length Δt:

$$1/2\ V_p\ \Delta t = I'_{dc}\ R(T - \Delta t) \tag{6.8}$$

where

$$T = 1/f = \text{line period}$$

Because the voltage waveform is $V(t) = \sqrt{2}\ V_1 \sin \omega t$, $dV/dt = \sqrt{2}\ V_1\ \omega \cos \omega t$. It follows that:

$$V_p = \sqrt{2}\ V_1\ \omega\ \Delta t = 533\ V_1\ \Delta t \tag{6.9}$$

$$V_p = \frac{2\ \sqrt{2}\pi\ V_1\ \Delta t}{T} \tag{6.10}$$

Thus, Equation (6.9) may be written as

$$\sqrt{2}\ \pi\ V_1 \left(\frac{\Delta t}{T}\right)^2 = I'_{dc}\ \ R\ 1\left(-\ \frac{\Delta t}{T}\right) \tag{6.11}$$

Because $\Delta t/T$ will generally be much less than 1, it follows:

$$\left(\frac{\Delta t}{T}\right)^2 - \frac{I'_{dc}\ \ R}{\sqrt{2}\ \pi\ V_1}$$

or

$$\frac{\Delta t}{T} = 0.474 \sqrt{\frac{I'_{dc}\ R}{V_1}} \tag{6.12}$$

From Equations (6.10) and (6.12), it follows:

$$V_p = 4.21\ V_1 \sqrt{\frac{I'_{dc}\ R}{V_1}} = 4.21 \sqrt{V_1\ I'_{dc}\ R} \tag{6.13}$$

The current waveform through R will be as shown in Figure 6-6. The RMS value of this current will be (triangle only):

$$I'_{rms} = \frac{1}{\sqrt{3}}\ 4.21 \sqrt{V_1\ \frac{I_{dc}}{R}} \sqrt{\frac{\Delta t}{T}} \tag{6.14}$$

Using Equation (6.12)

$$I'_{rms} = 1.67 \sqrt{\frac{V_1\ I'_{dc}}{R}} \left(\frac{I'_{dc}\ R}{V_1}\right)^{1/4} \tag{6.15}$$

$$I'_{rms} = 1.67\ V_1^{1/4}\ R^{-1/4}\ I'_{dc}{}^{3/4} = 1.67 \left(\frac{V_1}{R}\right)^{1/4} I'_{dc}{}^{3/4} \tag{6.16}$$

The total RMS, including the I'_{dc} portion is:

$$I_{rms} = I'_{dc} \left[1 + \frac{1.67}{I'_{dc}{}^{1/4}} \left(\frac{V_1}{R}\right)^{1/4} \right] \tag{6.17}$$

Because

$$R = 1/2\ V_1^2/P,\ R = \frac{R'\ V^2}{2P}$$ where R' is per-unit (pu) value.

$$\frac{I_{rms}}{I_{rating}} = \frac{I_{dc}}{I_{rating}} \left[1 + 1.67 \left(\frac{2 I_{rating}}{R' I_{dc}} \right)^{1/4} \right] \quad (6.18)$$

Letting $I_{dc}/I_{rating} = \lambda$ (per unit dc current) and letting $\alpha = I_{rms}/I_{rating}$ (per unit rms),

$$\alpha = \lambda \left[1 + 1.98 \left(\frac{\lambda}{R'} \right)^{1/4} \right] \quad (6.19)$$

where R' is the per-unit resistance in both the transformer and source.

Plotting Equation (6.19) for various values of R' yields Figure 6-7. Notice that R' does not have a large impact on the steady-state RMS primary current unless it is an order of magnitude less than the values shown. Such a value is unrealistic and in general will not occur.

Figure 6-9 shows the R = 0.02 per-unit (pu) case duplicated for alpha but also shows the time to fuse failure for a 10 kVA 4800:240V dedicated transformer installed with a 5E fuse. Even under worst conditions it takes at least 3 s for the fused cutout to open. As the transformer becomes larger, the time to open becomes longer because the amount of dc that can be injected by one PV unit as a percentage of transformer kVA (λ) becomes smaller (i.e., 10 kW on a 25 kVA transformer yields λ = 0.4).

C. EFFECTS OF DC INJECTION ON DISTRIBUTION TRANSFORMERS

Sections 6.1 and 6.2 present a quantitative answer to the question of time to saturation and time to outage (blown fuse). In each analysis, conservative assumptions were made that shortened the time of interest rather than lengthening the result. Table 6-1 summarizes the results.

This table shows that even under worst conditions, a 10-kVA distribution transformer with a 10 kW PV injecting 10 kW of dc power, a control system has seconds to operate, i.e. to clear the condition before the primary fused cutout will open, causing a loss of service.

Table 6.1 Time to Outage ($R = 0.02$; $X = 0.05$; $\gamma = 0.30$)

λ	Δt_{sat}, s	α	Δt_{blow}, s
0.05	1.1119	0.174	
0.10	0.556	0.396	
0.15	0.369	0.641	
0.20	0.275	0.904	
0.25	0.218	1.181	
0.30	0.181	1.469	
0.35	0.154	1.767	
0.40	0.134	2.075	
0.45	0.118	2.391	
0.50	0.106	2.714	
0.55	0.096	3.044	
0.60	0.087	3.385	1000
0.65	0.080	3.723	700
0.70	0.074	4.071	200
0.75	0.068	4.425	10
0.80	0.064	4.784	7
0.85	0.060	5.147	4
0.90	0.056	5.515	3
0.95	0.053	5.888	2.7
1.00	0.050	6.265	2.5

D. RELATIVE SATURATION OF TRANSFORMERS

A concern still exists concerning the effects of saturation on small load transformers. To understand this concern, the value of H_{dc} is evaluated for two transformers of similar design, one small and the other large. Because the issue of concern involves a load transformer versus a distribution transformer, the analysis considers the effects upon these transformers when they are placed in parallel. As in previous analyses, conservative assumptions will be made throughout the analysis.

Assume $P = K_1 W_a A_c$ where W_a is window area and A_c is core area. This assumes constant core flux and current density:

$$P = K_1 W_a A_c$$

Because proportions are assumed fixed, it follows:

$$W_a = K_1 A_c$$

and

$$P = K_1 K_2 A_c^2$$

$$A_c = P/K_1 K_2$$

Because the gap, lg, scales as a linear dimension and any linear dimension scales as A_c, it follows that

$$l_g = K_3 P^{1/4}$$

For fixed voltage and flux levels, the number of turns, N, varies inversely with the core cross section.

$$N = K_4/A_c = K_5/P$$

The dc current will be given by Ohm's Law:

$$I_{dc} = V_{dc}/R$$

The dc resistance is proportionate to the length per turn times the number of turns divided by the cross section of each turn:

$$R = \frac{K_6 (A_c)^{1/2} (N)}{(W_a/N)}$$

After manipulation

$$R = K_7 P^{-5/4}$$

Finally,

$$\frac{N\ I_{dc}}{l_g} = K_8 V_{dc} P$$

Therefore, as the power rating and size of a transformer is increased, the value of NI_{dc}/l_g will increase as will the flux offset due to the impressed dc voltage. Thus, the larger transformer, the pole-top distribution transformer, should saturate before the load transformer.

E. SATURATION CONCLUSIONS

The results from this section conclusively show that a finite time exists before saturation will occur for a normally loaded distribution transformer. Following saturation, a period of seconds transpires before the primary fused cutout of the distribution transformer opens. This "window of control" should be sufficient to allow sensing and operation of a control function that will prevent saturation of the distribution transformer. Furthermore, because this transformer will saturate before any load transformers placed in parallel, the above control action will also be sufficient to prevent damage to customer load transformers.

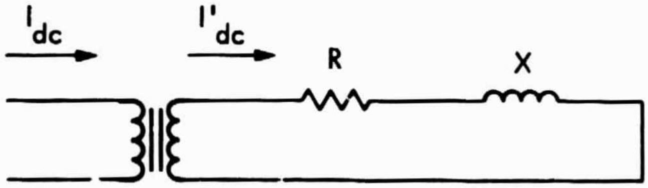

Figure 6-1. Analysis Circuit

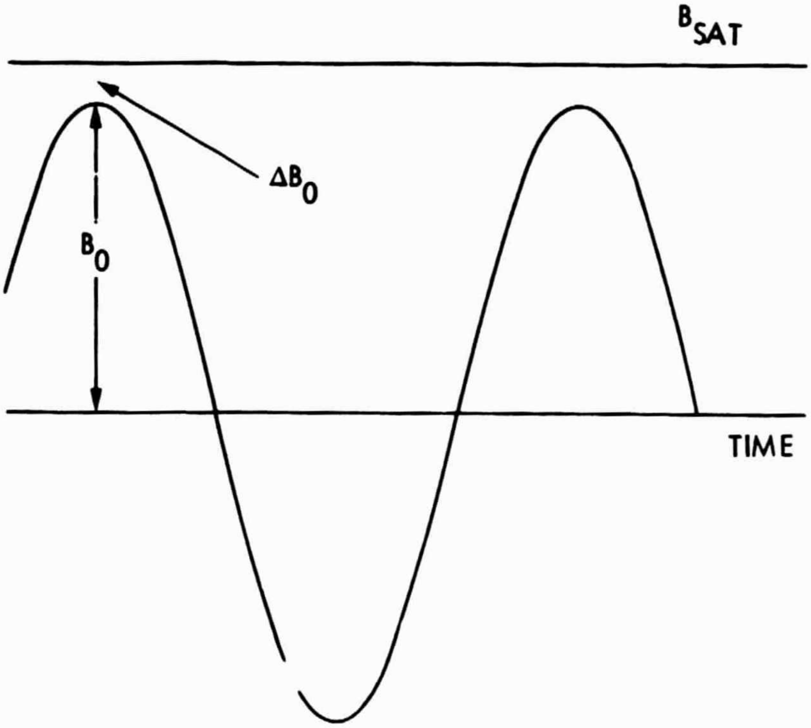

Figure 6-2. Margin Before Saturation is Attained

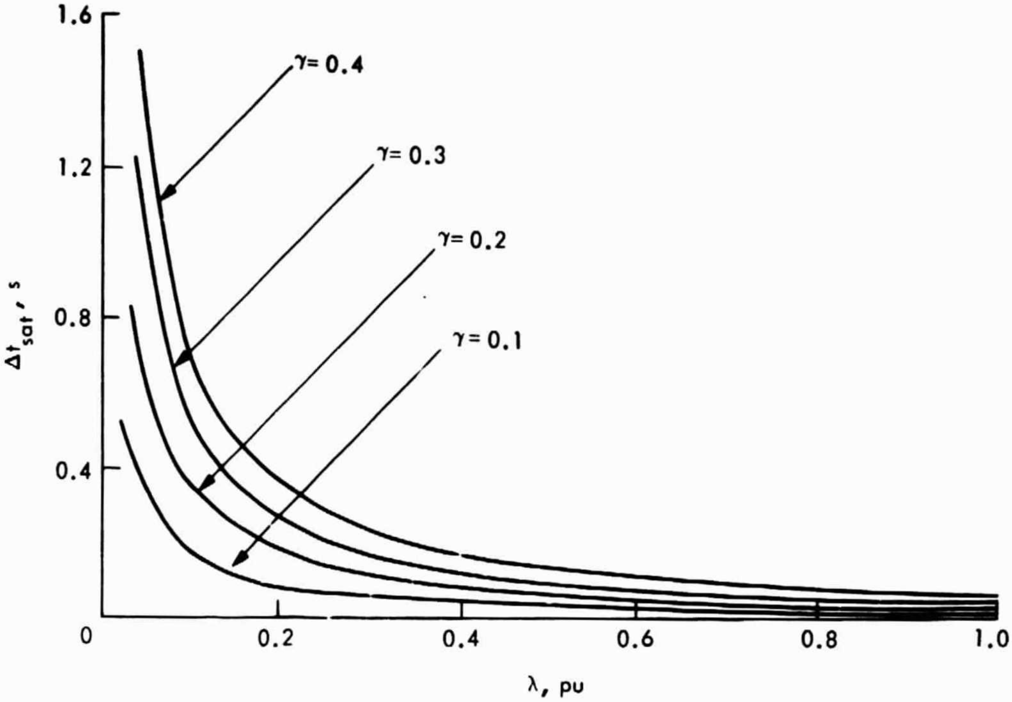

Figure 6-3. Time to Saturation for Varying Injected Power and Saturation Margin

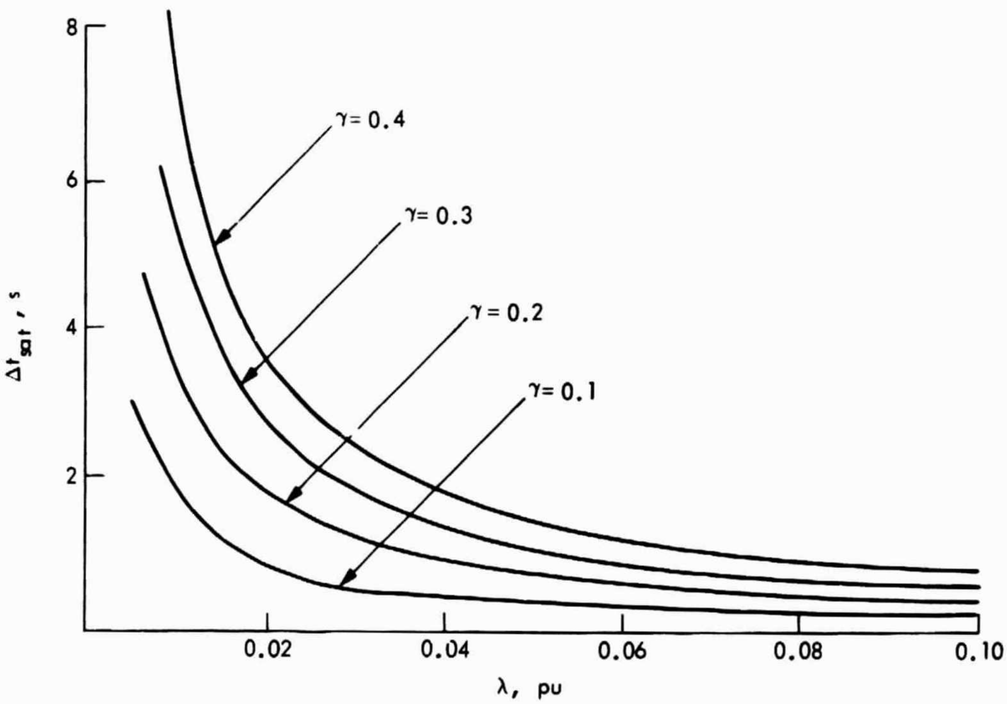

Figure 6-4. Time to Saturation for Low Values of Injected Power

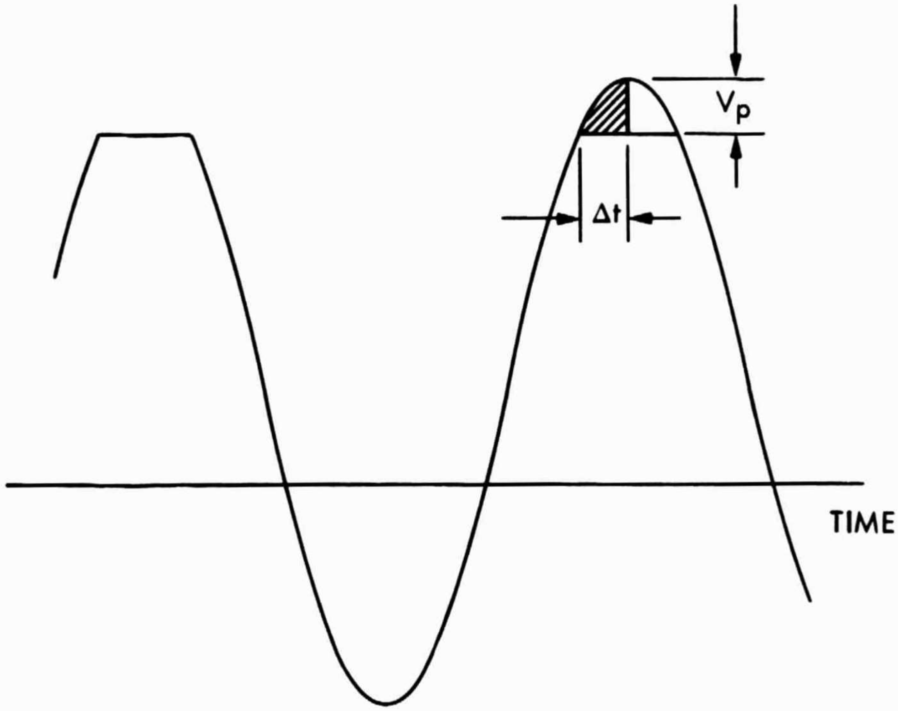

Figure 6-5. Core Flux vs. Time After Saturation

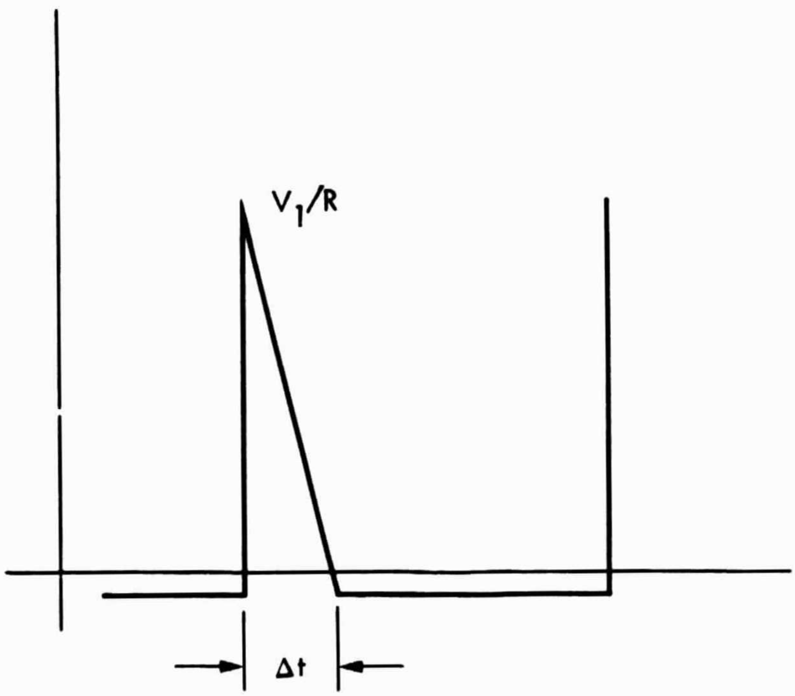

Figure 6-6. Current vs. Time Through Resistor R

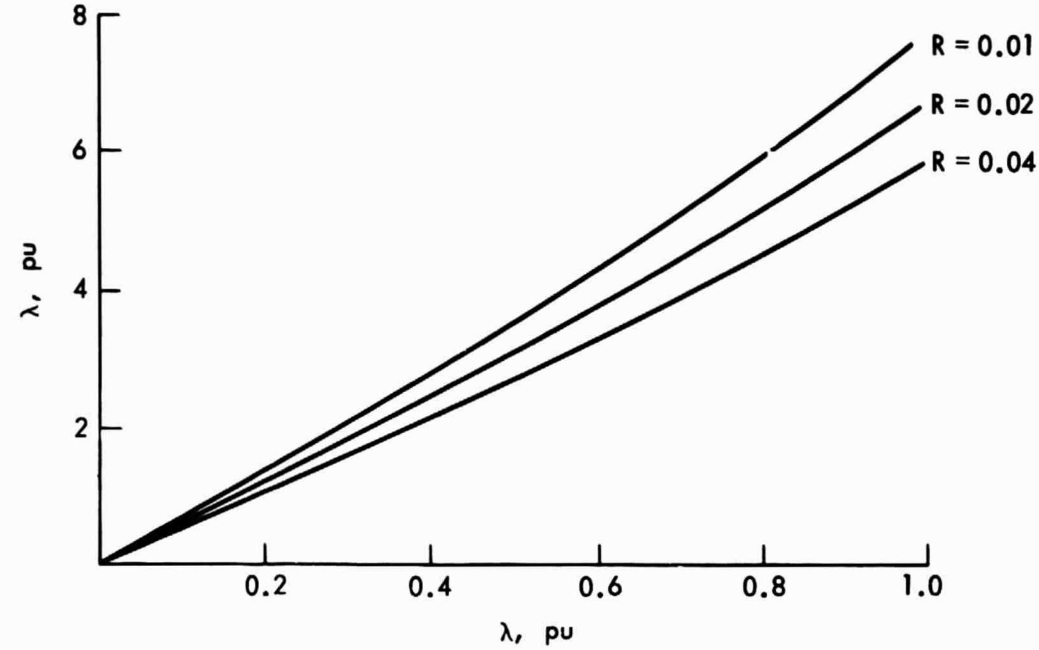

Figure 6-7. Steady-State rms Current Following Saturation for Various Injected Powers and Utility Resistance Values

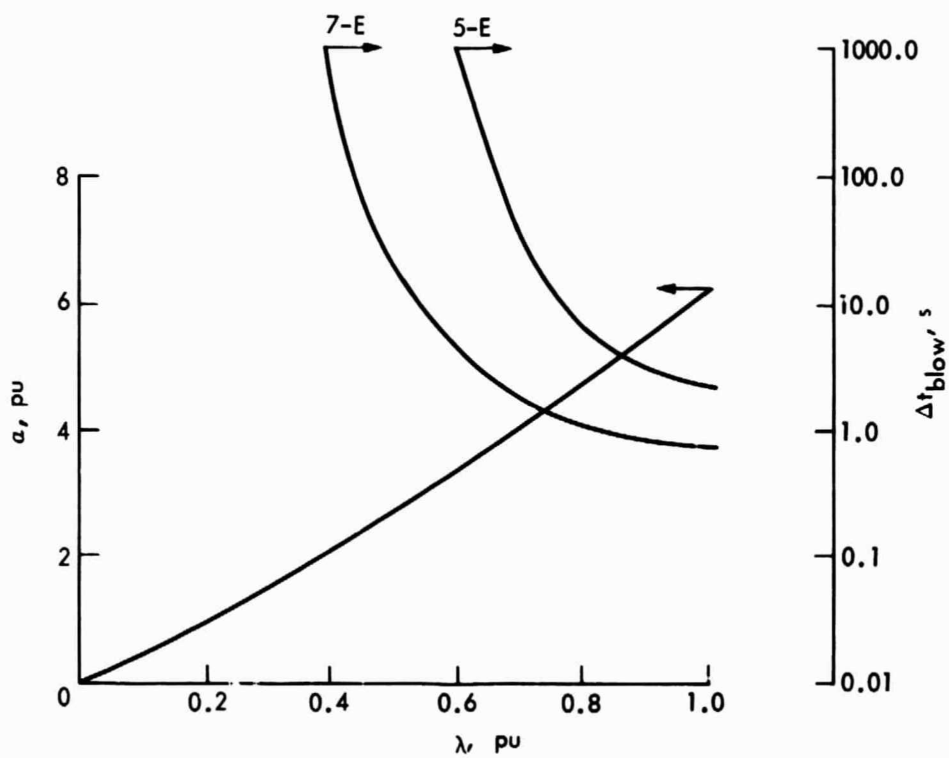

Figure 6-8. Time to Fuse Failure (Δt_{blow}) for Various Injected Powers

SECTION VII

RECOMMENDATIONS

The previous sections have set forth data for a Transformer Power Conditioner Subsystem (TPCS) detailing concerns and methods to alleviate or meet those concerns. This section will draw that material together by developing a set of recommendations concerning:

(1) The wiring of the PV system to the utility that alleviates grounding concerns.

(2) The wiring of the PV system that alleviates customer load concerns.

(3) The topologies most suitable for inclusion in a TCPS.

(4) A set of control requirements that negate the concerns of dc injection.

The recommendations in this section are not an exclusive set; other options are available. The proposed recommendations attempt to show how the above issues interplay and yet meet the concerns of utilities, consumers, and manufacturers. It is left to others to perform the expanded analyses that will determine the "best" design, components, and equipment for a TPCS.

A. UTILITY CONNECTION REQUIREMENTS

After a review of the appropriate sections of the NEC guidelines (Section 3), the schematic of Figure 7-1 was developed. The visible disconnect, meter, and shunt trip circuit breaker are shown separately for clarity. A more detailed wiring diagram is shown in Figure 7-2. This circuit will meet the safety, grounding, and isolation concerns as long as the control requirements of Subsection VII-C are used.

The system connection involves a three-wire twisted line to the power conditioning unit, with a fourth, non-current carrying ground wire for case grounding of the PCS. The service drop, service equipment, and distribution transformer are shown. Such a configuration eliminates any concerns for customer load saturation (as discussed in Section IV).

The array has been center tapped to ensure minimum voltage to ground, lessening the concerns about personnel safety and keeping the critical maximum voltage to less than 600 Vdc. A lightning spark gap or arrestor is installed at the array to provide a path to ground for lightning surges (as suggested in Section III).

The power conditioning unit itself is shown as a black box because its selection can facilitate dc isolation but in and of itself is not the only means for isolation.

Sensors S1 and S2 measure critical dc levels and are used in conjunction with a shunt trip circuit breaker CB1 to prevent destructive dc injection. The dc crowbar is used to remove all dc from the circuit breakers in a fashion described in Subsection VII-C. This combination of grounding and control will meet the concerns of the NEC guidelines and meet the isolation concerns of the utility. The selection of proper inversion techniques enhances these issues.

B. TOPOLOGY SELECTION

Information is available concerning the four topologies under consideration. Table 7-1 incorporates this information into a set of criteria that can be qualitatively evaluated.

Table 7-1. Topology Evaluation[a]

Criteria	Dual Pre-regulator Bridge	Modulated Bridge	Ćuk Pre-regulator Bridge	GE High-Frequency Bridge
Small magnetic size (mass)	+	+	-	-[b]
Low magnetic losses	+	+	-	-[b]
Magnetic simplicity	+	+	-	-[b]
Flexible operation (input/output limits, low voltage array)	-	-	+	±
Circuit complexity	+	+	-	-
Small input ripple	-	-	+	-
Unbalanced operation allowed	-	-	+	+
Low crossover distortion	-	+	-	-
Low voltage stresses	-	-	+	+
Low current stresses	+	+	-	-
Limited dc injection following PCS fault	-	-	+	+

[a]+ is positive attribute; - is negative attribute.
[b]Includes interstage transformer.

An analysis of Table 7-1 reveals the following:

(1) The Cúk and GE circuits have similar characteristics.

(2) The modulated and dual pre-regulator bridge circuits have similar characteristics.

However, the choice of the "best" topology is never this simple; engineering judgment must be used.

Between the Cúk and GE circuit, the modified Cúk circuit should have better efficiency as well as lower overall mass and size even though the Cúk inductor design is slightly more complex. It should also have lower overall mass and size. The major difference between the Cúk and the GE circuits is that the Cúk circuit has a continuous buck-boost capability whereas the GE circuit is fixed after the transformer turns ratio has been chosen.

Between the other two circuits, the choice is not so straightforward. The simplicity of the modulated bridge, which many times implies increased reliability, and the lack of crossover distortion indicate the superiority of the modulated bridge circuit. While it is true that the component voltage stresses are slightly higher for the modulated bridge, current technology should be able to meet these requirements.

Thus, the designer is left with a choice between the modified Cúk and the modulated bridge topologies. Two factors of the Cúk circuit allow it to be used in a more flexible fashion. First, the coupling capacitors ensure that no dc current from the array will be injected into the distribution transformer, even if the protection circuit should fail. The topology still has the same constraint as all topologies, in that a fault in the output bridge will impose a dc load onto the distribution transformer, causing possible saturation. Secondly, because the modified Cúk circuit has a continuous buck-boost capability, any array voltage can be used to deliver power to the utility and local loads. This is not the case with other circuits in which the array voltage must be maintained above a certain minimum value. For the GE circuit, this minimum is determined by the interstate transformer upon design. For the other two circuits, the array voltage must be maintained higher than the worst-case peak utility line voltage. Although the system can be designed to overcome this problem upon installation, degradation of the array over time can cause the dc voltage to drop below the minimum utility line voltage. Such a condition will prevent the proper operation of these two circuits.

If the coupling capacitor or array-voltage issues are of little concern to the designer, then the modulated bridge wins out due to its simplicity. However, the operating flexibility of the Cúk circuit, its fail-safe dc injection mode, and its allowance for unbalanced operation, seem to offset any engineering and construction complexities and may lessen utility concerns about dc injection.

C. CONTROL REQUIREMENTS

For the circuit of Figure 7-2 to operate in a proper fashion, certain requirements are placed on the sensors, the circuit breaker, and the dc crowbar:

(1) Sensors S1 and S2 must sense dc injection values of 3% of the secondary current at a sensitivity of 0.1% (The sensitivity relates to a value of about 50 mA of dc current for a small distribution transformer).

(2) Upon sensing this value, CB1 must operate within 3 s to remove the source of the dc from the distribution transformer, thus excluding the possibility of primary fused cutout opening due to dc injection.

(3) Simultaneously, or shortly thereafter, the dc crowbar must be closed to remove any dc for the circuit breakers.

These requirements allow the following features: with the placement and operation of the crowbar, CB1 can be an ac circuit breaker sized to interrupt full load ac current (not full load dc current). At these ratings, this is a substantial savings in cost to the consumer. The crowbar is an inexpensive and reliable device.

These requirements have also removed a faulted PV source from the utility. However, to obtain the maximum energy for the source, the PV source should be interconnected as much as possible to the utility, implying automatic restart. Most utility requirements on this matter require a full checkout of the cause of the fault. Such a manual checkout will indoubtably involve separation of the array and PCS. However, this will not remove the source from the crowbar. Thus, a commutation circuit is required to commutate current out of the dc crowbar.

Similarly, if automatic restart is allowed, a commutation circuit also must be required to commutate current out of the dc crowbar. Following this procedure, normal restart may be initiated. In the extreme case where three failures to restart the system have occurred, the system shall be taken off line and manually checked out.

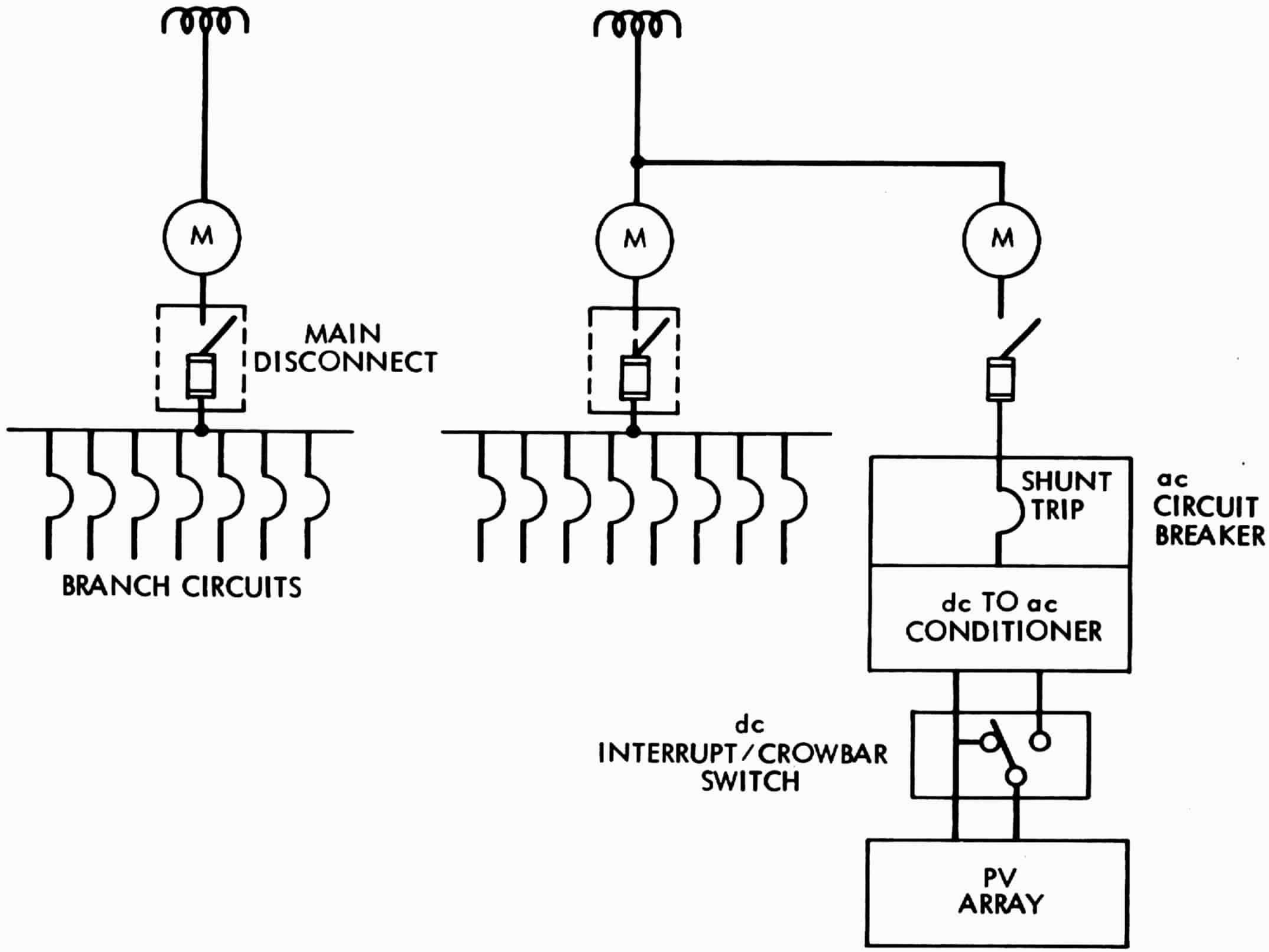

Figure 7-1. One-Line Diagram for Interconnection of Photovoltaic System to Utility

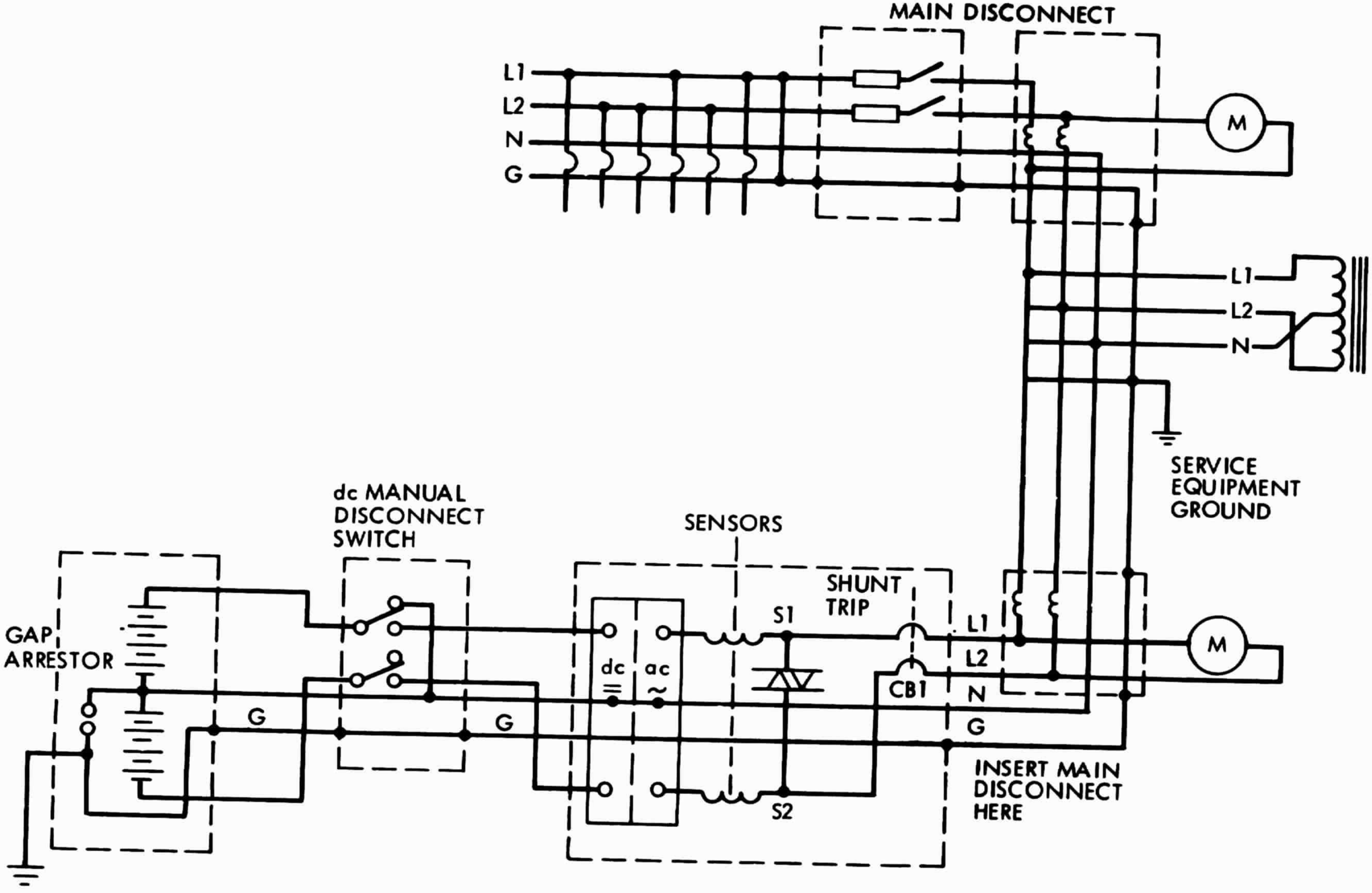

Figure 7-2. Detailed Schematic for Interconnection

SECTION VIII

CONCLUSIONS

This report addresses the issues surrounding the use of an isolation transformer and possible solutions to the problem areas. Table 8-1 summarizes these areas and their possible solutions:

(1) Current Utility Practices. Current utility practices vary from utility to utility. The specific requirements upon the PV installer are not specific. Some utilities require isolation transformers while others prefer the use of dedicated distribution transformers to solve perceived problems. The discussions and analyses presented in this report tend to negate these concerns. Each concern is reviewed and a possible solution is presented.

(2) Direct Current Injection. The principal issue associated with a TPCS involves the question of dc Injection. After detailed analysis, it was found that a finite amount of time transpired from the failure of the PCS until (1) saturation of the distribution transformer occurred and (2) the primary fused cutout would open, if at all. The solution of this problem involves the development of a control system that senses dc injection and operates a contactor and crowbar internal to the TPCS.

(3) Customer Transformers (Saturation). A second issue involves the effect of a TPCS on customer transformers (saturation). Because two-wire systems (in which the single-phase load is connected between a hot leg and ground) lead to average value dc injected into the customer load, a three-wire connection for the inverter is recommended.

(4) Ground Loops. Ground loops are always a concern in any installation. The various applicable codes are quite specific about requirements. Because lightning protection and solid grounding are required at the array and because the code allows for grounding physically remote but electrically close to the array, a current carrying neutral tied to the house ground is recommended. To provide lightning protection, a spark gap or lightning arrestor is used that only grounds the array under transient conditions.

(5) Safety. Personnel safety is another issue addressed by the study. To reduce the array voltage to ground that a consumer or maintenance personnel might contact, a three-wire array connection with current carrying neutral (see discussion under Ground Loops) is recommended. Ground Fault Interrupters (GFIs) are not required by code for single-phase PV installations.

Table 8-1. Issues and Solution Summary

Concern	Study Findings	Solution
Direct Current Injection of Distribution Transformer	Finite time to saturation Finite time to fuse open	Sense 1% 0.1% sensitivity 3 s to contact open crowbar array concurrently
Customer Load Saturation	Two-wire connection leads to average value dc on customer loads	Three-wire connection for inverter
Ground Loops	Code requires lightning protection	Current carrying neutral tied to house ground
	Code requires solid array grounding	Lightning arrestor ties array to ground at array
	Code allows array grounding at meter pan	
Safety	Excessive array voltage	Three-wire dc array connection with current carrying neutral
Current Utility Practices	Guidelines not specific Isolation transformer may be required	Array connection, control schemes will negate need for isolation transformer
	Dedicated transformer is preferred usage	Inverter connection, control scheme negate need for dedicated transformer
Multiple Ground Paths	Interference between customers	Control scheme eliminates interference
Multiple Customers on one Utility Transformer	Increased outages	Control scheme reduces outages
	Increased customer complaints	Control scheme reduces customer complaints

(6) Optimum Topology. The issue of optimum topology is one for the designer of the TPCS system. If complete flexibility is required in the installation of interest, then a topology like the Cuk circuit would be applicable where dc injection is prohibited due to the topology, and any array voltage is accommodated due to the buck nature of the circuit. If, on the other hand, the array voltage is designed to exceed the worst-case utility line voltage and simplicity of design is desired, then the modulated bridge might be a wise choice. The choice of an optimum design must be left to the TPCS designer.

Once these issues have been resolved, they must be re-examined in light of the possibility of multiple users on a single utility distribution transformer. The issues here include increased outages and complaints due to interference and transients from the PV source, multiple ground loops between residences, and the use of a dedicated distribution transformer to alleviate these concerns. The array connections and control schemes discussed in this report negate the need for such additional utility equipment. By controlling the dc injection, the ground loop paths, and the transient conditions of the PCS, little reference, if any, will be seen between customers.

In conclusion, a transformerless PCS can be developed that will meet all the concerns of all parties involved. It should have characteristics that please the consumer and manufacturer; it should be safe, highly efficient, and cheaper to build and buy. At the same time, a transformerless PCS will meet the necessary requirements of the utilities who wish to protect themselves and other non-PV customers.